Bulletin of Engineering Geology and the Environment (2022) 81: 213
https://doi.org/10.1007/s10064-022-02718-8

ORIGINAL PAPER

The effect of metamorphism on the aggregate properties of gabbroic rocks

Cindy Urueña[1] · Charlotte Möller[1] · Jenny Andersson[2] · Jan-Erik Lindqvist[3] · Mattias Göransson[2]

Received: 30 October 2021 / Accepted: 17 April 2022 / Published online: 28 April 2022

Abstract

Granitic rocks are durable materials sought after for the production of road and railroad aggregates. Granitic bedrock commonly, however, includes gabbroic components, which may enhance or decrease the aggregate performance. This study evaluates the variation in resistance to fragmentation (Los Angeles value, LA) and wear/abrasion (micro-Deval value, M_{DE}) for the fraction 10/14 mm of gabbro in different metamorphic states. Samples were collected along a 150-km profile where metamorphic conditions grade from epidote–amphibolite to high-pressure granulite-facies, and the degree of metamorphic recrystallization varies with the amount of hydrous fluid. Rocks with no or incipient metamorphic recrystallization preserving their primary igneous fabric and interlocking texture meet the criteria for both asphalt base course and track ballast in railroad, with LA and M_{DE} values below 25% and 14%, respectively. Mafic granulite and fine-grained amphibolite have LA values below 25% and can be used in unbound layers. Mafic granulites crystallize at high temperatures but commonly preserve a relict igneous texture due to limited hydration. Coarse-grained amphibolite and migmatitic amphibolite have the poorest performance. They recrystallized at hydrous conditions, leading to complete recrystallization, grain coarsening, and loss of interlocking igneous texture. This study shows that both temperature and infiltration of hydrous fluids significantly affect the technical properties. Even at high metamorphic temperatures, gabbroic rocks may yield aggregates of high technical performance. At hydrous conditions, however, recrystallization results in rock aggregates suitable for unbound layers only. The variation in metamorphic grade and hydration is easily assessed by the geologist in the field and by using standard petrographic microscopy.

Keywords Crushed rock aggregates · Gabbroic rocks · Los Angeles · Micro-Deval · Metamorphic recrystallization

Introduction

Crushed rock aggregates are raw materials used for the construction of roads, railroads, and concrete. Technical tests of aggregate materials are routinely performed to provide quantitative data on their functionality. The resistance to fragmentation and the resistance to wear are important properties for aggregates to be used for road and railroad; these properties are commonly measured as Los Angeles value (LA) and micro-Deval value (M_{DE}), respectively. In turn, these properties are steered by the relative mineral abundances and texture, the latter measured as grain size, grain size distribution, grain morphology, and grain boundary complexity (Åkesson et al. 2001; Lindqvist et al. 2007; Tavares and das Neves 2008; Sajid et al. 2016; Hemmati et al. 2020).

Within metamorphosed bedrock regions, i.e., most mountain belts and shield areas, the mineral assemblage and texture of a rock are governed by the metamorphic conditions during the latest stage of recrystallization. These metamorphic conditions include pressure, temperature, availability and composition of fluids, and deformation. Despite the potential of metamorphic petrology in prospecting for high-performance aggregates, metamorphic conditions and type of

✉ Cindy Urueña
cindy.uruena@geol.lu.se

Charlotte Möller
charlotte.moller@geol.lu.se

Jenny Andersson
jenny.andersson@sgu.se

Jan-Erik Lindqvist
linerikjan@gmail.com

Mattias Göransson
Mattias.Goransson@sgu.se

[1] Department of Geology, Lund University, Lund, Sweden

[2] Geological Survey of Sweden, Uppsala, Sweden

[3] Research Institutes of Sweden – RISE, Lund, Sweden

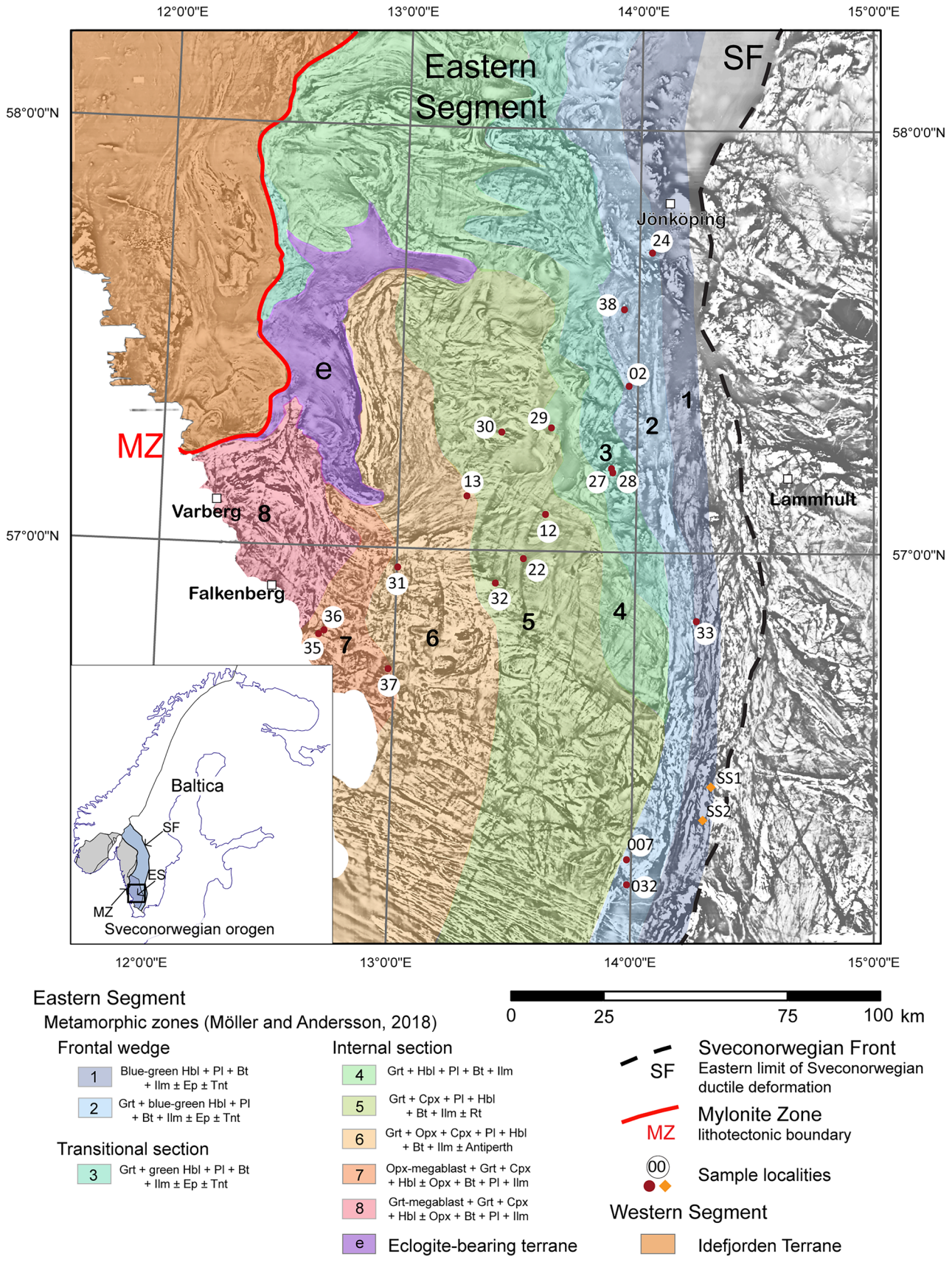
12°0'0"E
13°0'0"E
14°0'0"E
15°0'0"E
58°0'0"N
57°0'0"N
Eastern Segment
SF
MZ
e
Jönköping
Varberg
Falkenberg
Lammhult
8
7
6
5
4
3
2
1
24
38
02
30
29
13
27
28
12
22
31
32
36
35
37
33
SS1
SS2
007
032
Baltica
SF
ES
MZ
Sveconorwegian orogen
Eastern Segment
Metamorphic zones (Möller and Andersson, 2018)
Frontal wedge
1 Blue-green Hbl + Pl + Bt + Ilm ± Ep ± Tnt
2 Grt + blue-green Hbl + Pl + Bt + Ilm ± Ep ± Tnt
Transitional section
3 Grt + green Hbl + Pl + Bt + Ilm ± Ep ± Tnt
Internal section
4 Grt + Hbl + Pl + Bt + Ilm
5 Grt + Cpx + Pl + Hbl + Bt + Ilm ± Rt
6 Grt + Opx + Cpx + Pl + Hbl + Bt + Ilm ± Antiperth
7 Opx-megablast + Grt + Cpx + Hbl ± Opx + Bt + Pl + Ilm
8 Grt-megablast + Grt + Cpx + Hbl ± Opx + Bt + Pl + Ilm
e Eclogite-bearing terrane
0 25 75 100 km
SF Sveconorwegian Front
Eastern limit of Sveconorwegian ductile deformation
MZ Mylonite Zone
lithotectonic boundary
00 Sample localities
Western Segment
Idefjorden Terrane

◂**Fig. 1** Metamorphic zones of the Eastern Segment with sample locations (in red numbered dots, orange dots for samples of group 0). The metamorphic zones illustrate an increasing metamorphic grade from < 600 °C in the east to ≥ 800 °C in the west, as recorded from assemblages in Fe–Ti–rich metagabbro. The west-dipping Mylonite Zone (MZ, red line) is the lithotectonic boundary between the Eastern Segment and the western Sveconorwegian terranes, with the Idefjorden Terrane (shaded orange) positioned structurally immediately above the Eastern Segment. The Sveconorwegian Front (SF) marks the eastern limit of Sveconorwegian ductile deformation and metamorphic recrystallization. Figure modified from Möller and Andersson (2018)

recrystallization are rarely considered key factors influencing the technical properties of the aggregates.

In a previous publication (Urueña et al. 2021), we investigated correlations between metamorphic conditions and technical properties (LA and M_{DE} values) in granitic rocks. Samples of similar chemical compositions were collected along a 150-km long profile in which metamorphic conditions grade from epidote–amphibolite-facies to high-pressure granulite-facies. The results demonstrated that the technical properties of granitic rock aggregates improve both with lower metamorphic temperature and lower H_2O conditions. The general reason for these correlations is that temperature and amount of H_2O control the macro- and micro-textures via different metamorphic deformation and recrystallization processes for quartz and feldspars.

Gabbroic rocks are common constituents of the bedrock in many geologic environments. By making up parts of crushed rock aggregates, they can improve or deteriorate the bulk aggregate functionality. Gabbroic rocks undergo pronounced changes of their main mineral assemblage during metamorphism—an important difference with respect to granitic rocks that are dominated by the recrystallization mode of the pre-existent minerals, quartz, K-feldspar, and plagioclase. Therefore, for metagabbroic rocks, aggregate properties are expected to vary significantly with the metamorphic conditions and are different from that of granitic rocks. In this paper, we investigate the interplay between metamorphic conditions and aggregate functionality of metamorphosed gabbroic rocks (including dolerites) along the same metamorphic profile as that investigated by Urueña et al. (2021).

Geological setting and sample locations

The investigated area is located in the Eastern Segment of the Sveconorwegian Province in SW Scandinavia (Fig. 1). It represents a part of the Fennoscandian continent that underthrusted tectonic units west thereof and underwent regional metamorphism and deformation during a syn- to late-collisional stage of the Sveconorwegian orogeny 990–960 Ma ago (Möller et al. 2015; Möller and Andersson 2018; Bingen et al. 2020). The protoliths of the metamorphosed Eastern Segment rocks are dominantly c. 1.7 Ga granite (with subordinate quartz monzonite, granodiorite, and quartz monzodiorite) and younger intrusions, c. 1.6, 1.4, and 1.2 Ga, of gabbro, granite, and syenite (e.g., Söderlund et al. 2005; Stephens and Wahlgren 2020). The protoliths of these rocks are partly well-preserved in the easternmost Sveconorwegian Province, where deformation and metamorphism were non-penetrative.

The investigated mafic rocks were originally emplaced as dolerite dikes and gabbro bodies. Several generations of mafic intrusions have been identified in the Eastern Segment: 0.97–0.94 Ga Blekinge–Dalarna dolerites that mark post-collisional extension following the Sveconorwegian orogeny; c. 1.22 Ga mafic intrusives associated with syenite and minor anorthosite; c. 1.40 Ga intrusions that are associated to the Varberg charnockite, granite, and minor anorthosite; and c. 1.57 Ga dolerite and gabbro (Värmland hyperites; Wahlgren et al. 1996; Söderlund et al. 2005; Brander et al. 2011; Beckman et al. 2017). In addition, the Frontal wedge of the Eastern Segment includes mafic dike swarms dated at 1.27 Ga (the Moslätt dolerites, belonging to the Central Swedish Dolerite Group; Brander et al. 2011) and at 1.42 Ga (the Axamo dikes; Lundqvist 1996). The area around Jönköping (Fig. 1) also exposes 1.47–1.44 Ga massif-type anorthosite, leucogabbro, and gabbro (the Jönköping anorthosite suite; Brander and Söderlund 2009). Few of the many metamorphosed gabbro and dolerite bodies in the internal parts of the Eastern Segment have been dated for their protolith ages.

Based on the mineral assemblages in metagabbroic rocks, Möller and Andersson (2018) defined eight metamorphic zones from epidote–amphibolite-facies in the east to high-pressure granulite-facies in the west. (Fig. 1; Table 1). The metamorphic conditions across these zones are estimated to range from c. 600 °C at mid-crustal conditions to c. 800 °C and 10 kbar, the latter corresponding to 35–40 km depth. The metamorphic zones have been defined based on key mineral assemblages in non-migmatitic metagabbro (zones 1–6) and peritectic minerals in migmatitic metagabbro (zones 7 and 8), respectively (Table 1; no. of localities = 287). In gabbroic rocks, the key assemblages were formed under relatively dry conditions. Each zone also hosts amphibolite bodies metamorphosed under higher H_2O contents. The hydrated rocks contain higher modal amounts of hornblende and may lack one or several of the anhydrous index minerals garnet, clinopyroxene, and orthopyroxene. For this reason, "plain" hornblende- and plagioclase-dominated amphibolite is present locally in all eight zones. In zones 4–8, where the temperature was high enough (~ 650 °C and above), the presence of free H_2O initiated partial melting, which is the reason for that migmatitic amphibolite formed in these zones.

Table 1 Key mineral assemblages of metagabbroic rocks in the Eastern Segment, from Möller and Andersson (2018)

Zone	1	2	3	4	5	6	7	8
Metamorphic assemblages in non-migmatized metagabbro								
Blue-green hornblende	X	X	(X)					
Epidote	X	X	X					
Titanite	X	X	X	X				
Plagioclase	X	X	X	X	X	X	X	X
Fe-Ti-oxide	X	X	X	X	X	X	X	X
Garnet		X	X	X	X	X	X	X
Green hornblende			X	(X)				
Olive-green hornblende				X	X	X	X	X
Rutile				(X)	(X)	(X)	(?)	(X)
Clinopyroxene					X	X	X	X
Antiperthite						X	X	X
Orthopyroxene						X	X	X
Mineral blasts in leucosome in migmatitic garnet amphibolite								
Garnet, 0.5–2 cm				X	X	X	X	X
Orthopyroxene, 2–10 cm							X	X
Clinopyroxene, 0.5–3 cm								X
Garnet, 4–20 cm								X

Nineteen samples were collected across the Eastern Segment (Fig. 1) for comparison of the technical properties of metagabbroic rocks of different metamorphic character. Five main rock types were targeted: (A) near-pristine gabbro, (B) metagabbro with relict igneous texture, (C) non-migmatitic amphibolite, (D) migmatitic amphibolite, and (E) mafic granulite. Petrography and technical test data of four additional samples have been included, from which technical test values are available: one sample of near-pristine gabbro (group A) and one of metagabbro with relict igneous texture (group B) from the Geological Survey of Sweden (MGO080007A, GS_007 and MGO080032, GS_032) and two samples of unmetamorphosed dolerite/gabbro (group 0) by courtesy from Scandinavian Stone. The technical values of the selected samples presented in this paper are representative for their specific rock type and thereby for the comparison of different metamorphosed gabbro varieties. We emphasize that the technical values reported herein are not representative of the composite products of individual quarries.

Methods

Sampling

The targets of this study were medium- to coarse-grained (c. 2–10 mm) gabbro and their metamorphic equivalents. The sampled rocks are from freshly blasted outcrops in active or abandoned quarries and road cuts. The twenty-three samples cover the variations of metamorphic conditions in the Eastern Segment from unmetamorphosed to high-grade conditions (Fig. 1, Tables 1 and 2, Online Resource 1). Weathered or hydrothermally altered rocks were not included in the study. In the text and tables, sample naming is referenced by numeric code without the CU19-prefix (see complete sample information in Online Resource 1).

At each locality, c. 80 kg of fresh rock were sampled. Twenty-five to thirty-five kilograms were used for aggregate functionality tests, 5–20 kg for bulk geochemical analysis, and a hand sample for thin section preparation and reference.

Petrographic analysis

Petrographic analysis involves determination of the rock's constituent minerals, texture, and fabric elements. The definitions of the three terms microstructure, fabric, and texture partly overlap. Fabric is defined as the spatial and geometrical configuration of the grains, crystals, or pores in rocks (Higgins 2006). In metamorphic petrology, texture involves many different geometrical aspects such as grain size and shape, interlocking features, and coronitic texture. Microstructures refer to the spatial grain-scale features as grain boundaries, mineral arrangement, and lattice-preferred orientation (Passchier and Trouw 2005).

Petrographic and microstructural analysis of thin sections included qualitative and quantitative analysis of

Table 2 Summary of investigated samples and their mineral constituents, divided into groups based on their petrographic characteristics (see main text for details). Mineral abbreviations follow Whitney and Evans (2010). Minerals are listed in the order of abundance

Sampling group	Sample code	Locality	Met. zone	Rock-type description	Igneous minerals	Corona minerals	Metamorphic minerals
Group 0: Pristine gabbro	SS1	Diabase quarry	1	Pristine gabbro, medium grained	Pl, Opx, Opq	n.o	n.o
	SS2	Diabase quarry	1	Pristine dolerite, grain size variations locally	Pl, Opx, Bt, Opq	n.o	n.o
Group A: Near-pristine gabbro	02A	Mjogaryd quarry	3	Near-pristine isotropic gabbro, medium-grained	Pl, Opx, Opq, Bt, Ol, Ap, (Cpx)	Opx, Amp, Grt, Bt, Opq (Cpx)	Very fine-grained, in coronas
	28	Herrestad incip. quarry	3	Near-pristine isotropic gabbro, medium- to coarse-grained	Pl, Opx, Ol, Bt, Ap, (Cpx)	Opx, Amp, Grt (Cpx)	Very fine-grained, in coronas
	33	Målaskog roadcut	1	Near-pristine isotropic gabbro, medium- to coarse-grained	Pl, Ol, Bt, Opx, Cpx, Opq, (Kfs), Ap	Opx, Amp, Grt, Bt, Opq (Cpx)	Very fine-grained, in coronas
	38	Bondstorp roadcut	3	Near-pristine isotropic gabbro, medium-grained	Pl, Cpx, Opx, Ol, Bt, Ap, (Kfs)	Opx, Amp, Grt, Bt	Very fine-grained, in coronas
	GS_007	Gumlösa quarry NE of Hässleholm	2	Near-pristine isotropic gabbro, medium-grained	Pl, Opx, Cpx, Opq	Cpx, (Opx) Hbl, Bt	Very fine-grained, in coronas
Group B: Metagabbro w relict igneous texture	02B	Mjogaryd quarry	3	Metagabbro with relict igneous texture	Textural relics of Pl, Px, Opq	n.o	Hbl, Pl, Bt, Grt, Qtz, Ep
	27	Herrestad roadcut	3	Metagabbro with relict igneous texture	Pl, relics of Cpx and Opq	n.o	Hbl, Pl, Grt, Qtz, Bt
	GS_032	Sjunkaröd, SE of Hässleholm	2	Metagabbro with relict igneous texture	Pl, relics of Cpx and Opq	n.o	Hbl, Grt, Pl, Bt
Group C: Amphibolite	24	Sandseryd quarry	2	Amphibolite, medium-grained	n.o	n.o	Hbl, Pl, Bt, Qtz, Opq
	29	Anderstorp roadcut	4	Amphibolite, fine-medium-grained, linear fabric	n.o	n.o	Hbl, Pl, Bt, Opq, Qtz, Ttn, Opq
	31B	Bökås quarry	6	Amphibolite, fine-medium-grained	n.o	n.o	Hbl, Pl, Bt, Qtz, Opq, Grt
	30	Gransjön roadcut	5	Amphibolite, fine-grained	n.o	n.o	Hbl, Pl, Qtz, Cpx, Opq, Grt
	32B	Bäck quarry	6	Amphibolite, fine-grained	n.o	n.o	Hbl, Pl, Cpx, Qtz, Opx, Grt, Opq
Group D: Migmatitic amphibolite	12C	Kållerstad quarry	5	Garnet-poor migmatitic amphibolite	n.o	n.o	Hbl, Bt, Qtz, Pl, Opq, Ttn, Grt, Aln
	22	Nickelsbo quarry	5	Garnet-rich migmatitic amphibolite	n.o	n.o	Hbl, Pl, Grt, Bt, Qtz, Opq, Ttn, Rt
	35	Stockabacka (old quarry)	7	Opx-megablast-bearing garnet-rich migmatitic amphibolite	n.o	n.o	Hbl, Pl, Qtz, Grt, Cpx, Bt*, Scap*, Opq
	37	Tippakull roadcut	6	Opx-megablast-bearing garnet-rich migmatitic amphibolite	n.o	n.o	Hbl, Pl, Grt, Qtz, Bt, Opq, Rt

Table 2 (continued)

Sampling group	Sample code	Locality	Met. zone	Rock-type description	Igneous minerals	Corona minerals	Metamorphic minerals
Group E: Mafic granulite	13B	Rökla quarry	6	Garnet- and clinopyroxene-rich metagabbro	n.o	n.o	Hbl, Pl, Grt, Cpx, Qtz, Bt, Opq
	13C	Rökla quarry	6	Garnet- and clinopyroxene-rich metagabbro	n.o	n.o	Grt, Hbl, Cpx, Pl, Qtz, Bt, Opq
	32C	Bäck quarry	6	Garnet- and clinopyroxene-rich metagabbro	Textural relics of igneous Cpx	n.o	Cpx, Grt, Qtz, Pl, Bt, Opq, Opx
	36	Bårarp quarry	7	Garnet- and clinopyroxene-rich metagabbro	n.o	n.o	Cpx, Grt, Pl, Bt, Opq, Opx, Hbl, Qtz

n.o: not observed
* = altered mineral

mineral assemblages and textures, using a standard polarizing optical microscope (Olympus, BX51) with an integrated digital point counting system (PetroG). The modal proportions of minerals were quantified using point counting of 500 points per thin section. The microstructures were defined from relationships between the mineral phases, such as mineral intergrowths, reaction textures, exsolution textures (e.g., lamellae), fabric orientation, and crystal sizes and shapes. In rocks with complex textural relations, the mineral identification was supported by energy dispersive X-ray analysis (EDS, using AZTEC software by Oxford Instruments) coupled to a field emission scanning electron microscope (FE-SEM, Tescan Mira 3) at the Department of Geology, Lund University.

Grain size measurements and grain size distribution were determined for the non-migmatitic amphibolite samples (group C) using an image-based technique because of the variable technical values among this group. Polarized scanned thin section images were processed and converted into binary images to identify single crystals. The open-source program ImageJ (Rasband 1997) was used for automatic particles analysis. Input settings for the minimum size of the particles to be measured were set at 32.5 microns (variations in this parameter have a large impact on the proportion of the finest grain fraction). The grain size was defined by the Feret's diameter, i.e., the maximum length between two extreme points of the crystals. Bin ranges for size classification were defined as very fine-grained: < 0.125 mm, fine-grained: 0.125–0.25 mm, medium-grained: 0.25–1 mm, coarse-grained: 1–2 mm, and very coarse-grained: > 2 mm. It should be noted that this grain size classification is different from the standard used for field classification (very fine-grained < 0.1 mm, fine-grained 0.1–1 mm, medium-grained 1–5 mm, coarse-grained 5–10 mm, very coarse-grained > 10 mm).

Three types of microcracks (intracrystalline, trans-crystalline, and grain boundary cracks) were identified and examined with fluorescence microscopy. To quantify the cracks, we overlapped petrographic and fluorescent images in an area of 1.0 cm^2 and set traverse lines spaced at 0.1 cm forming a grid with a total length of 100 mm. The linear crack frequency was determined in four selected samples with a different microcracking degree. The resulting number of microcracks per millimeter was used as a reference value to determine the relative abundance of microcracks in the other samples.

Whole-rock geochemical analysis

Whole-rock geochemical analysis of major and trace elements of individual samples ($n = 19$) was performed by ALS Scandinavia AB. Description of analytical methods and data report are available in Online Resource 1.

Technical tests and density measurement

The aggregate functionality for road and railroad was assessed through two tests of the mechanical properties. Resistance to fragmentation was examined by a Los Angeles (LA) test (reference method: EN 1097–2) and resistance to wear by a micro-Deval (M_{DE}) test (reference method: EN 1097–1). Two steps of crushing and sieving were performed. Initial crushing was done in a rotational jaw crusher and followed by crushing in a smaller jawbreaker. Five fractions (0–10; 10–11.2; 11.2–14; 14–16; and > 16 mm) were obtained using a Gilson machine sieve. Fractions 10–11.2 mm and 11.2–14 mm were used for the LA and M_{DE} tests. A 5 kg sample was used for the LA test, and 1 kg of sample was split into two parts, 0.5 kg each, for a duplicate M_{DE} test. The technical methods followed the standard procedures and calculations detailed in Urueña et al. (2021). The results for LA and M_{DE} values are expressed in percentage by weight (wt%) and represent the loss of material in percent.

The density of the samples was measured by hydrostatic weighing of 600 g dry fraction sieved at 14-mm mesh. The density was calculated as the product between dry weight and the water density at room temperature ($\rho = 0.998$ g/cm^3), divided by the difference in weight between the dry and wet sample (procedure detailed in Urueña et al. 2021).

Sample descriptions and general petrography

The rocks included in this study are gabbro with variable metamorphic overprint (Table 2). Rocks that fully or partly preserve a primary igneous texture are in this paper collectively referred to as gabbro or metagabbro categories. Rocks that consist of a hornblende- and plagioclase-dominated assemblage are referred to as amphibolite or, where leucosome-bearing, migmatitic amphibolite. Rocks dominated by metamorphic clinopyroxene, garnet, and plagioclase are termed mafic granulite.

Group 0: Pristine gabbro (n = 2; metamorphic zone 1)

Samples in this group (SS1 and SS2) are predominantly homogeneous gabbros from 25 to 100-m wide N-S elongated dolerite intrusions in the easternmost part of the Frontal Wedge. These rocks are dark gray, isotropic, and even-grained (Fig. 2a). They have a well-preserved igneous texture and mineralogy with 2–3-mm-long plagioclase laths, forming a sub-ophitic texture (Fig. 2b, d). The dominant minerals are plagioclase, intergrowths of orthopyroxene and clinopyroxene, and Fe-Ti oxides (Fig. 2c, d), with lesser amounts of olivine and biotite. Both pyroxene and plagioclase grains have a clouded brownish appearance caused by abundant minute inclusions of Fe-Ti oxide. Variations in the large intrusions include pockets of igneous gabbro pegmatite and, locally, domains affected by metamorphic fluid infiltration with amphibole rims on pyroxene and fine-grained biotite rims on Fe-Ti oxides.

Group A: Near-pristine gabbro (n = 5; metamorphic zones 1–3)

In the field and hand specimen, group A rocks are dark gray to pitch black and seemingly pristine igneous gabbroic rocks (Fig. 3a). They have an isotropic texture with randomly oriented plagioclase laths. Most samples are on the average medium-grained, with grain sizes up to 6 mm; however, in the samples from Herrestad (28) and Målaskog (33), grain sizes of plagioclase reach 8 and 10 mm, respectively. The rocks are dominated by igneous olivine, pyroxenes, lath-shaped plagioclase, opaque minerals (dominantly Fe-Ti-oxide), reddish biotite, and abundant small grains of accessory apatite (Fig. 3c–f). One sample, from Gumlösa (GS_007), does not contain olivine. In all rocks, plagioclase is dark.

Investigation under the petrographic microscope and SEM reveals that the plagioclase is darkened due to clouding of minute opaque inclusions of Fe-Ti-oxide (cf. Estifanos et al. 1997). Pyroxene and olivine grains are in a similar fashion clouded by minute opaques.

The near-pristine gabbros are not completely unaffected by metamorphism. All rocks have thin, c. 50–200-µm-wide coronas consisting of very fine-grained minerals surrounding dark minerals (Fig. 3b). Olivine is surrounded by double coronas dominated by colorless orthopyroxene (inner) and green amphibole (outer), with the minerals growing in a radial pattern. The inner corona also contains tiny needles of opaques (occasionally spinel) and vermicular biotite. The outer corona includes occasional biotite and opaques. Fe-Ti-oxides are rimmed by double coronas of biotite (inner) and green amphibole (outer). Igneous biotite grains are rimmed by coronas of very fine-grained biotite. Garnet is present in the coronas in four of the samples, most commonly in coronas around Fe-Ti-oxides and/or biotite (Fig. 3g, h).

Group B: Metagabbro with relict igneous texture (n = 3; metamorphic zones 2–3)

The metagabbroic rocks of group B have relict igneous texture with partly preserved igneous minerals. The metamorphic overprint is easily seen in the field and hand specimen by the greenish tint of dark mineral domains, the presence of very-fine-grained garnet, and the light color of plagioclase (Fig. 4a). Thin sections show that pyroxene grains are partly to completely replaced and surrounded by fine-grained metamorphic amphibole of variable color (Fig. 4c–h).

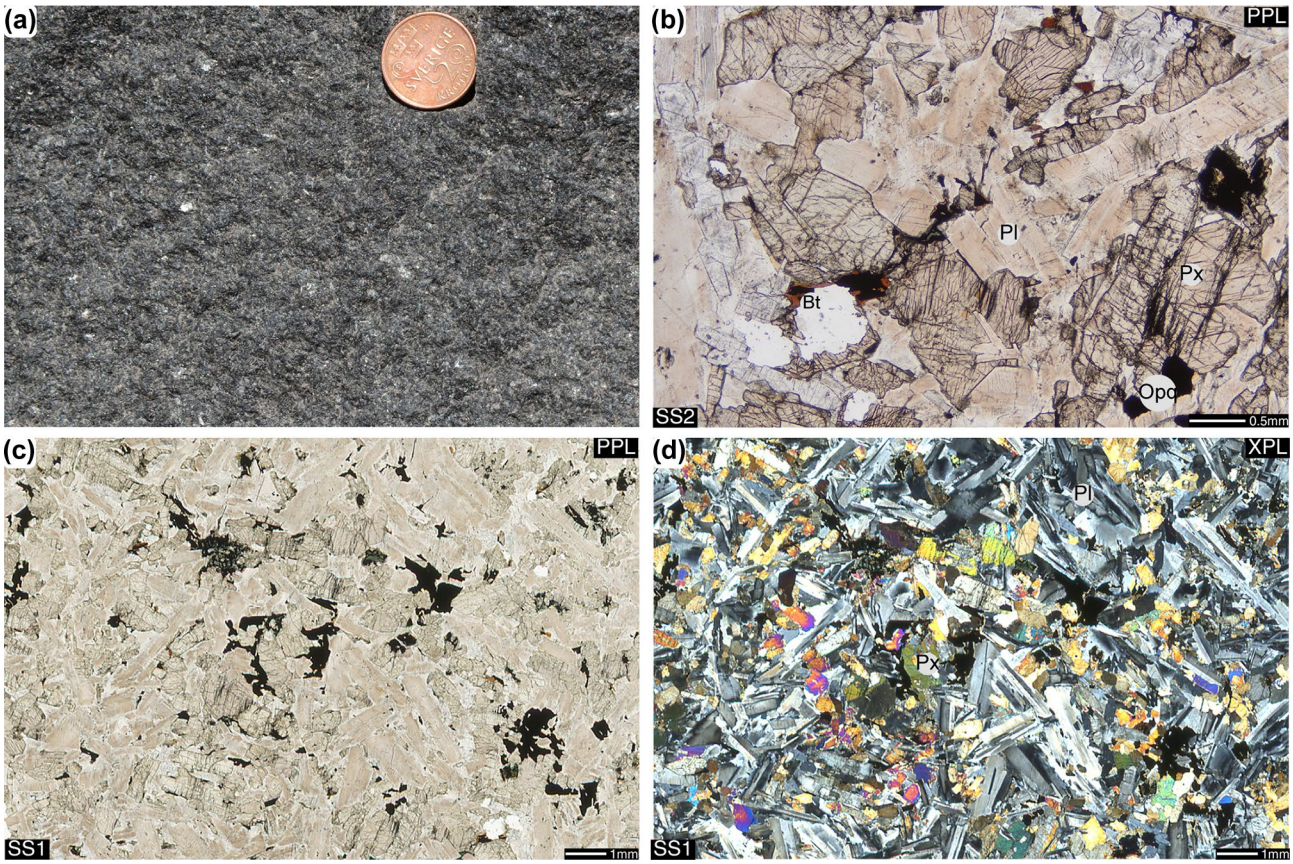

Fig. 2 Pristine gabbro (group 0): field appearance, photomicrographs, and scanned thin sections. **a** Dark gray, medium-grained dolerite, representative of pristine gabbro. **b** Photomicrograph (plane-polarized light, PPL) of unmetamorphosed dolerite with brownish clouded plagioclase, pyroxene, opaques, and biotite. **c** and **d** Thin section overview in plain light (PPL; **c**) and crossed polars (XPL; **d**) of dolerite with interlocking plagioclase laths (clouded brownish in PPL, gray tones in XPL), igneous pyroxene, and Fe-Ti oxides

Fe-Ti-oxide grains are partly replaced by fine-grained biotite aggregates developing a vermicular texture (Fig. 4b). Garnet is abundant and forms c. 0.5-mm-wide coronas between the dark minerals and plagioclase; locally, garnet forms 1-mm large crystals (Fig. 4g, h). Plagioclase is variably recrystallized: igneous clouded plagioclase is preserved in samples from Herrestad and Sjunkaryd (27 and GS_032; Fig. 4e, f), while plagioclase in the sample from Mjogaryd (02B) is largely recrystallized and contains abundant epidote/zoisite (Fig. 4c, d).

Group C: Amphibolite (n = 5; metamorphic zones 2–6)

Amphibolite samples in group C have in common that, macroscopically, the rocks are black and dominated by metamorphic hornblende and plagioclase. No igneous minerals are preserved. The amphibolites vary in grain size from fine- to medium-grained (0.5–3 mm) and texture (Fig. 5).

The amphibolite from Sandseryd (24) contains green pleochroic hornblende, plagioclase, brown biotite, and small amounts of opaque minerals. It is the most coarse-grained sample in group C, with a grain size of up to 3 mm and non-complex grain boundaries (Fig. 5c, d). The texture is isotropic, near-granoblastic to decussate. The amphibolite from Anderstorp (29) is also fine- to medium-grained but, in contrast to the Sandseryd sample, has a strong linear fabric defined by the orientation of biotite and amphibole (Fig. 5a, b). The amphibolite from Bökås (31B) has an isotropic texture and is different in that it bears garnet, with strongly anhedral shape, and has highly irregular grain boundaries. It is also somewhat finer-grained, with few grains exceeding 1 mm.

The samples from Bäck (32B) and Gransjön (30) differ from the other amphibolite samples in that they represent former mafic granulites (i.e., group E rocks) that have become amphibolitized. They are also finer-grained with individual grains averaging 0.1–0.2 mm (Fig. 5e, f). Both samples have linear deformation fabrics defined by oriented hornblende crystals. In the sample from Bäck, the lineation is also defined by oriented mineral aggregate domains rich in either hornblende or plagioclase, a texture reflecting an original medium-grain size of the gabbroic protolith.

Metamorphic garnet and pyroxene form small and strongly anhedral crystals in both the plagioclase- and hornblende-dominated domains. Plagioclase-rich felsic domains also include non-twinned and locally microperthitic K-feldspar and fine-grained anhedral quartz with lobulated grain boundaries and undulous extinction. Apatite, epidote, and titanite are accessory phases.

Group D: Migmatitic amphibolite (n = 4; metamorphic zones 5–7)

On a macroscopic scale, the migmatitic amphibolite samples can be divided into three types (Fig. 6): garnet-poor (Kållerstad, 12C), garnet-rich (Nickelsbo, 22), and garnet-rich with orthopyroxene megablasts (Stockabacka, 35, and Tippakull, 37, both from metamorphic zone 7).

Garnet-poor migmatitic amphibolite from Kållerstad (12C) is medium-grained hornblende- and plagioclase-dominated foliated rock with an average grain size of 1–3 mm (Fig. 6a). Under the microscope, lens-shaped, olive-green hornblende crystals form elongated aggregates intergrown with biotite and minor opaque minerals. These dark mineral domains form an anastomosing foliation together with elongated leucocratic domains that consist of plagioclase and quartz and are interpreted as leucosome (Fig. 6b). The leucocratic domains have a finer grain size, ~ 0.1–1 mm, and a near-granoblastic texture and contain occasional larger (~ 2 mm) lens-shaped quartz crystals. Sparse garnet crystals are 1–2 mm long, strongly anhedral, and allocated preferably in the leucocratic mineral domains.

Garnet-rich migmatitic amphibolite from Nickelsbo (22) is medium- to coarse-grained and rich in hornblende, plagioclase, and garnet (Fig. 6c). Under the microscope, olive-brown hornblende is intergrown with inequigranular plagioclase, both reaching c. 5 mm in size. Garnet forms subhedral, up to 6-mm-large grains. Grain boundaries are smooth and rounded. Biotite, opaques, and apatite occur in lesser amounts (Fig. 6d). Thin 3-cm-wide stromatic leucosomes of tonalitic composition are made up of quartz + plagioclase and small garnets.

Garnet-rich migmatitic amphibolite with orthopyroxene megablasts is a distinct rock type in the westernmost metamorphic zones (7 and 8 in Fig. 1), which consists of three distinctly separate components: mesosome, leucosome, and orthopyroxene megablasts up to 6 cm large (Fig. 6e). The mesosome is dark and fine-grained and consists of hornblende, plagioclase, garnet, and lesser amounts of clinopyroxene. Where well-preserved, orthopyroxene megablasts are black, commonly with minor brown staining along cleavage surfaces; these megablasts are situated within leucosome and are interpreted as a peritectic phase, i.e., formed by incongruent melting (Hansen et al. 2015). The orthopyroxene megablasts are typically surrounded by < 1-mm-wide rims of fine-grained garnet, hornblende + plagioclase intergrowths, and locally clinopyroxene + plagioclase intergrowths (Fig. 6f), which we interpret as formed during the crystallization of the leucosome, i.e., solid-state reaction between orthopyroxene and anorthite.

Two samples of this rock type are included in this study, from Stockabacka (35) and Tippakull (37). In sample 37, however, the orthopyroxene megablasts have been completely replaced by fine-grained aggregates of Fe-rich chlorite with some calcite and quartz, i.e., the products of low-grade metamorphic alteration. The pseudomorph also includes small crystals of amphibole.

Under the microscope, the mesosome consists of olive-green to olive-brown hornblende, pinkish garnet, plagioclase, and subordinate amounts of biotite and opaques; grain boundaries are smooth and rounded (Fig. 6g, h). Altered grains of biotite and scapolite occur throughout the mesosome (Fig. 6h). The tonalitic leucosome is medium-grained and consists of antiperthitic plagioclase and quartz (Fig. 6g). In the leucosome, the average grain size of plagioclase and quartz is significantly larger than in the mesosome, up to 5 mm, plagioclase is antiperthitic, and grain boundaries are highly irregular. Sparse small grains of hornblende and garnet are present in the leucosome.

Group E: Mafic granulite (n = 4; zones 6–7)

The mafic granulites of group E are all part of metadolerite bodies that range in width from c. 5 to 10 m. The sampled rocks are dark in color, lack signs of partial melting, and are rich in fine-grained garnet, especially abundant at the contact between dark and light mineral domains (Fig. 7). Inspection using a hand lens reveals that the dark mineral domains are rich in greenish gray clinopyroxene. The size of dark and light mineral aggregates, respectively, reflects the original grain size of the protolith gabbro (Fig. 7a). Two of the hand samples, from Rökla (13C) and Bäck (32C), indicate a protolith grain size of c. 5 mm. A second sample from Rökla (13B) indicates slightly finer grain size, and the sample from Bårarp (36) an even finer protolith grain size, of c. 2–3 mm. Except for sample 32B, the rocks have a deformation fabric (linear and/or planar) defined by alignment of the light and dark mineral aggregates (Fig. 7b–d).

Clinopyroxene is the predominant ferromagnesian phase in the samples from Bårarp (36) and Bäck (32C; Fig. 7b, c), and orthopyroxene is also present in these two samples. The amount of hornblende varies and reflects the uneven access to hydrous fluids during metamorphism. The sample from Bårarp (36) has a relatively low amount of hornblende, 4.5%, whereas the two samples from Rökla (13B and C) contain 40 and 22% hornblende, respectively (Figs. 7c–f

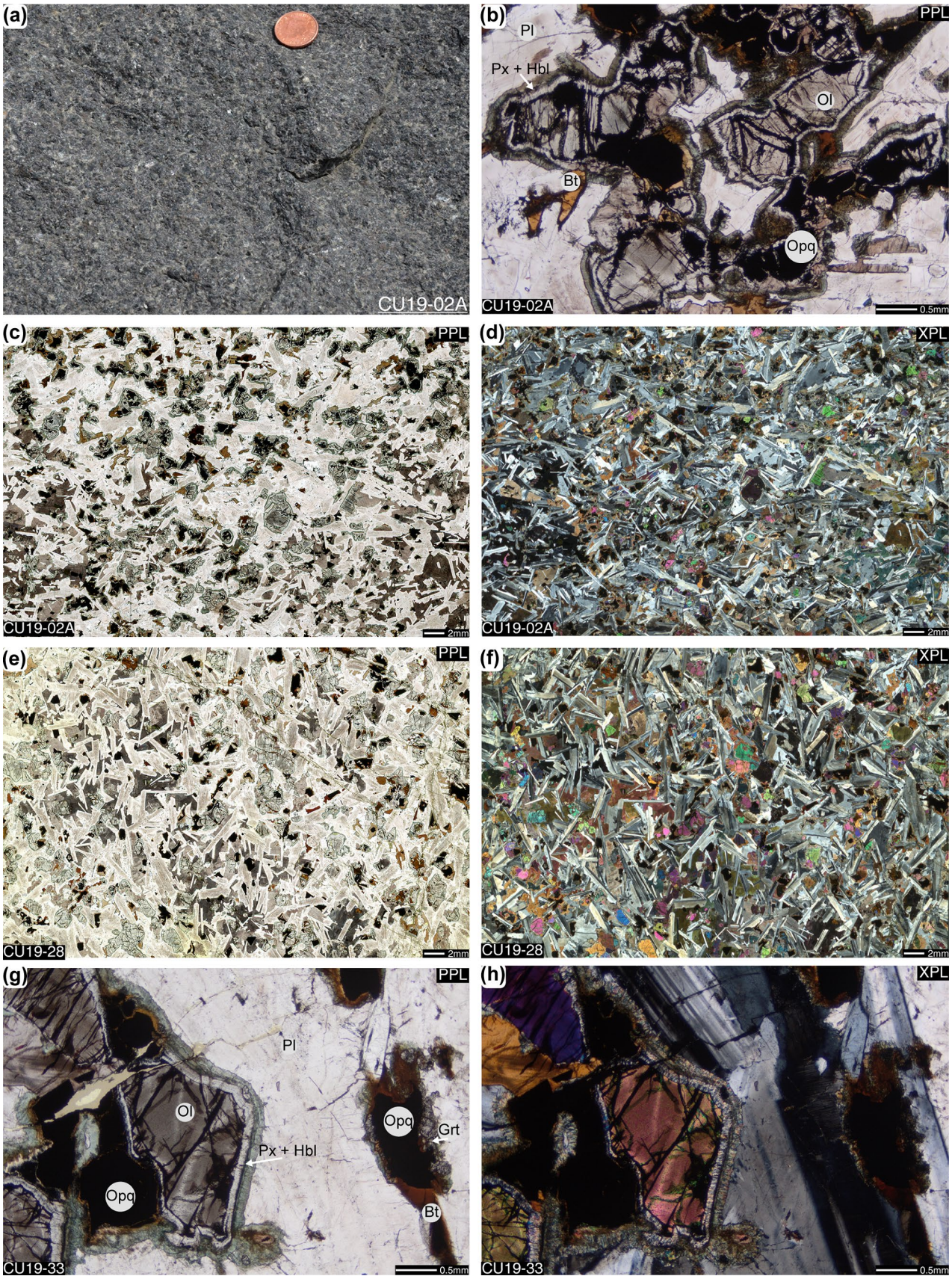
(a)
CU19-02A
(b)
PPL
Pl
Px + Hbl
Ol
Bt
Opq
CU19-02A
0.5mm
(c)
PPL
CU19-02A
2mm
(d)
XPL
CU19-02A
2mm
(e)
PPL
CU19-28
2mm
(f)
XPL
CU19-28
2mm
(g)
PPL
Pl
Ol
Opq
Grt
Px + Hbl
Opq
Bt
CU19-33
0.5mm
(h)
XPL
CU19-33
0.5mm

◂**Fig. 3** Near-pristine gabbro (group A): field appearance, scanned thin sections, and photomicrographs. **a** Pristine-looking gabbroic rock at Mjogaryd. **b** Photomicrograph (detail) of thin coronas around clouded igneous olivine, Mjogaryd. **c**–**f** Scanned thin section overviews of interlocking texture with igneous plagioclase pyroxene and Fe-Ti oxide in samples from Mjogaryd **c**–**d** and Herrestad **e**–**f**. **g**–**h** Photomicrographs (detail) of coronas in the sample from Målaskog. Olivine is rimmed by a double corona of orthopyroxene (inner) and amphibole (outer). Opaque rimmed by biotite and garnet (under plane and polarized light, respectively)

and 8a). The sample from Bäck (32C) is completely devoid of hornblende. Furthermore, this sample preserves up to 2-mm-large relics of igneous clinopyroxene in the core of dark mineral aggregates. The relics of igneous clinopyroxene are clouded by minute Fe-Ti-oxides and rimmed by clinopyroxene without clouding, either as clear rims or by aggregates of very fine-grained metamorphic neoblasts or both (Fig. 7g, h).

Felsic minerals, including plagioclase and subordinate amounts of quartz and K-feldspar, make up almost 30% of the rock volume. These minerals form polygonal aggregates of subhedral crystals with smooth grain boundaries (Fig. 7e, f). Usually, plagioclase shows well-developed albite twinning, and quartz has undulous extinction. Small non-twinned inclusions in plagioclase were identified as K-feldspar. Accessory minerals are apatite, zircon, and opaques.

Quantitative petrography

Mineral contents

The modal mineral proportions of all samples in the class groups A to E are summarized in a bar chart (Fig. 8a). Rocks of group A are dominated by plagioclase, reaching c. 50%. Anhydrous minerals, i.e., pyroxenes and olivine, sum to 30%. Igneous biotite and sparse hornblende make up < 10%, and quartz is absent. For rocks in group B, plagioclase makes up c. 30%, the quartz content ranges from 5–7%, and amphibole constitutes up to 30%. Clinopyroxene contents are variable, and garnet reaches 7–10%.

The mineral assemblages of the amphibolites in groups C and D are dominated by hornblende, with modal contents varying from 40 to 65%. Biotite contents are generally c. 10% but in one of the migmatitic samples is up to 17%. However, in the two fine-grained non-migmatitic amphibolites (samples 30 and 32B), biotite is in a very low content (< 1%). Garnet contents are variable but reach c. 16% in the migmatitic amphibolites (sample 37).

The mafic granulites are dominated by anhydrous ferromagnesian phases (garnet and pyroxenes) and plagioclase. Garnet reaches up to 30% and clinopyroxene almost 50 modal-%. One exception is the sample from Rökla (13B), where hornblende still prevails. Plagioclase contents are below 25%.

Grain size distribution of non-migmatitic amphibolites (group C)

The variable grain size and technical data (section "Technical test results") of samples in group C prompted quantitative grain size measurements. Cumulative and relative grain size distributions for these non-migmatitic amphibolites are illustrated in Fig. 8b. The grain size distribution curves of samples 30 and 32B show higher proportions of finer-grained fractions in these samples. A few coarser-grained domains in sample 32B have little effect on the total grain size distribution, and the medium-size fraction is comparable with the proportion in sample 30 (i.e., c. 20%). The highest percentages of very fine grains (≤ 0.125 mm) reach 35–41% in these samples.

The bar chart in Fig. 8c shows that coarser-grained amphibolites (samples 24, 29, and 31B) have a more homogeneous grain size distribution and contain lower amounts of fine-grained fractions.

Microcrack frequency

The relative frequency of microcracks for mafic rocks in groups A to E is arranged in four categories: very low, low, intermediate *(mid)*, and high (Table 3). The category *very low* includes rocks without microcracks or with a frequency below 0.04 microcracks/mm (measured in sample 31B). The category *low* includes samples with long trans-crystalline cracks that have a frequency up to 0.2 microcracks/mm (sample 29). The intermediate (*mid*) category is characterized by short length grain boundary microcracks, reaching up to 1 microcrack per mm (sample 13C). The samples with a *high* frequency of microcracks have up to 3.2 grain boundary cracks per mm, 1.9 intracrystalline cracks per mm, and 0.05 trans-crystalline cracks per mm (sample 22). Most of the intracrystalline microcracks occur in hornblende and garnet. Plagioclase is moderately affected by grain boundary microcracks, which occur in recrystallized domains only. However, the plagioclase in samples with very low and low frequencies of microcracks shows fluorescence, contrasting with non-fluorescent plagioclase in rocks with intermediate and high microcracking.

Bulk geochemistry

The range in chemical composition is narrow among the sampled rocks. The SiO_2 content varies between 44 and 49 wt%, and the X_{Mg} values are 2.6–5.2 wt%. The whole-rock

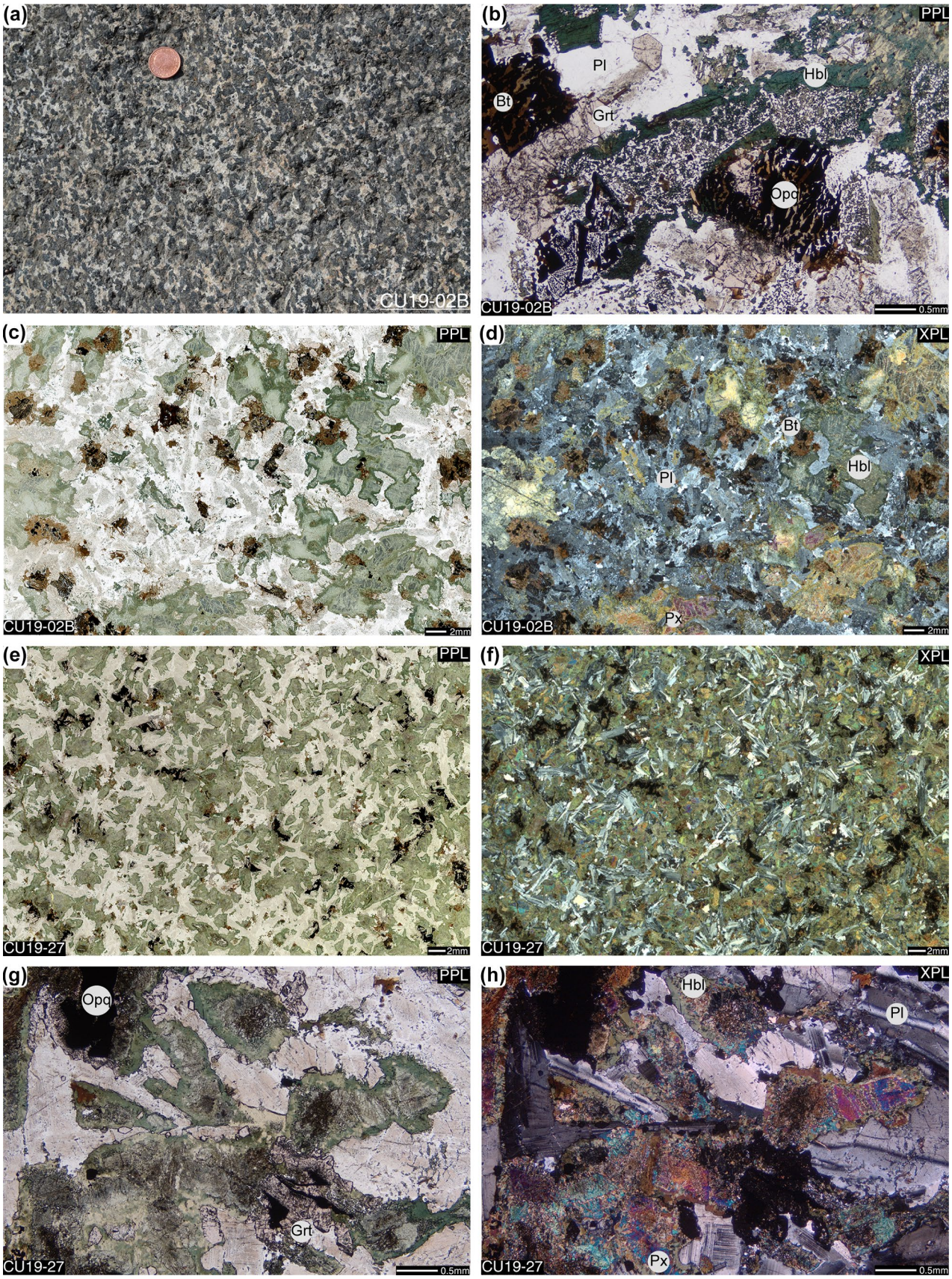
(a)
CU19-02B
(b)
PPL
Pl
Hbl
Bt
Grt
Opq
CU19-02B
0.5mm
(c)
PPL
CU19-02B
2mm
(d)
XPL
Bt
Pl
Hbl
Px
CU19-02B
2mm
(e)
PPL
CU19-27
2mm
(f)
XPL
CU19-27
2mm
(g)
PPL
Opq
Grt
CU19-27
0.5mm
(h)
XPL
Hbl
Pl
Px
CU19-27
0.5mm

◂**Fig. 4** Metagabbro with relict igneous texture (group B): field appearance, scanned thin sections, and photomicrographs. **a** Undeformed and partly recrystallized metagabbro at Mjogaryd, in which the igneous minerals have been replaced by greenish amphibole and white plagioclase. **b** Photomicrograph (detail) showing intergrowths of amphibole + plagioclase and biotite + opaques, surrounded by anhedral garnet. Plagioclase is colorless (without igneous clouding) and has abundant inclusions of very fine-grained zoisite. **c**–**f** Scanned thin section overviews of the textures in metagabbro at Mjogaryd **c**–**d** and Herrestad **e**–**f**. Relict igneous pyroxene grains are largely amphibolitized, and in **c**–**d**, the relict igneous plagioclase is largely recrystallized. **g**–**h** Photomicrographs (detail) of the metagabbro at Herrestad. Relict igneous clinopyroxene grains preserve exsolution lamellae in the cores, while the rims are replaced by hornblende. Garnet has preferentially grown around Fe-Ti oxides

geochemistry of these gabbroic rocks (Table 3) is presented in the R1-R2 diagram (De la Roche et al. 1980; Fig. 9a). The samples form a cluster covering the fields of gabbro and alkali-, syeno-, and monzogabbro. Samples in groups B, C, and D fall across the whole range, whereas the mafic granulites in group E plot in the gabbro field only. In the AFM diagram (Irvine and Baragar 1971; Fig. 9b) showing the ternary relations between $Na_2O + K_20$ (A), FeO_{tot} (F), and MgO (M), the samples assemble in the field of tholeiite series rocks except for one sample of migmatitic amphibolite (35) that plot on the boundary line to calc-alkaline rocks. This latter sample contains scapolite (Table 2).

The proportion of mobile elements can be affected by fluid ingress (in either an igneous or metamorphic stage) or partial melting (which normally results in melt loss and thereby of Na, K, Al, and Si). Any whole-rock alteration will also modify the metamorphic mineral assemblage and mineral chemistry. The whole-rock geochemical data were used to calculate the CIPW norm and assess possible alteration trends in whole-rock chemistry (Online Resource 1). The proportions between normative pyroxenes + olivine, normative plagioclase, and normative Fe-Ti oxides for the analyzed rocks are shown in Fig. 9c and depict the ideal mineralogy of the protolith. Most samples are grouped between 50 and 60% plagioclase, 10 and 30% pyroxene + olivine, and 20 and 30% Fe-Ti oxides (Fig. 9c). These minor variations indicated by the CIPW norm are observed within all groups, and there is no compositional distinction between high-grade metamorphic and near-pristine rocks. None of the samples has a leucocratic or ultramafic composition.

The relation between the immobile trace elements Zr and Ti usually remains unchanged despite metamorphic recrystallization and hydrothermal alteration of rocks. Figure 9d shows a plot of Ti versus Zr. The samples plot in a positive array with overlap between the different rock groups. One sample of orthopyroxene-megablastic migmatitic amphibolite (35) plots slightly below the positive trend described by the other analyses. This sample contains scapolite, which may point to element mobilization related to fluid ingress. Otherwise, metamorphosed rocks at higher conditions (i.e., the samples of migmatitic amphibolites and high-pressure granulites) plot along the same array as lower grade metamorphic and unmetamorphosed varieties. In summary, there appears to be no significant fractionation of the immobile elements Zr and Ti between near-pristine and high-grade metamorphic and migmatitic rocks.

Technical test results

Analytical data from density measurements, Los Angeles (LA), and micro-Deval (M_{DE}) tests are compiled in Table 3 and presented in Fig. 10. The diagram Fig. 10a shows LA versus M_{DE} test values with a classification of aggregate quality in road construction used by the Geological Survey of Sweden (Table 4; Mortensen and Göransson 2018). None of the mafic rocks in the Eastern Segment meets the requirements for class 1 aggregates suitable for all bound layers and paving. All rocks in groups 0, A, and B (i.e., pristine gabbro, near-pristine gabbro, and metagabbro with relict igneous texture) plot in class 2 (Fig. 10a). These rocks show the best suitability for the production of road aggregates with a range of LA values between 15 to 21% and M_{DE} values between 6 and 12.5%.

The rocks in groups C, D, and E are mainly distributed within the field of class 3, indicating poor technical performance, and these are only recommended for unbound layers. Noticeably, rocks recording the highest metamorphic conditions, corresponding to the high-pressure granulite facies (group E), have LA values between 17 and 22%, well below the threshold of 30% for classes 1 and 2, which stand for good resistance to fragmentation for these rocks. Nevertheless, the M_{DE} values of the group E rocks range from 15 to 22%, classifying them as class 3 aggregates unsuitable for bound layers.

Rocks penetratively recrystallized at non-migmatitic amphibolite facies conditions (group C) gave a wide range of LA and M_{DE} values, from 15 to near 50 in LA value and between 14 and 36 in M_{DE} value. Two fine-grained samples (amphibolitized mafic granulites) have LA values well below 30% (samples 30 and 32B). Sample 30 also has a low M_{DE} value of 13.8%, meeting the minimum requirement for a class 2 aggregate. All other samples fall in class 3, among which sample 31B has an exceptionally high M_{DE} value above 35% and sample 29 gives a LA value at near 50%.

The lowest resistance to fragmentation and wear is found among the migmatitic amphibolites (group D). Most samples have high LA value between 30 and 40% and M_{DE} values between 20 and 30%. One sample of garnet-rich migmatitic amphibolite (sample 22) yields extremely high LA and M_{DE} values (LA = 70.6% and M_{DE} = 35.5%). This rock type is unsuitable for road aggregate production.

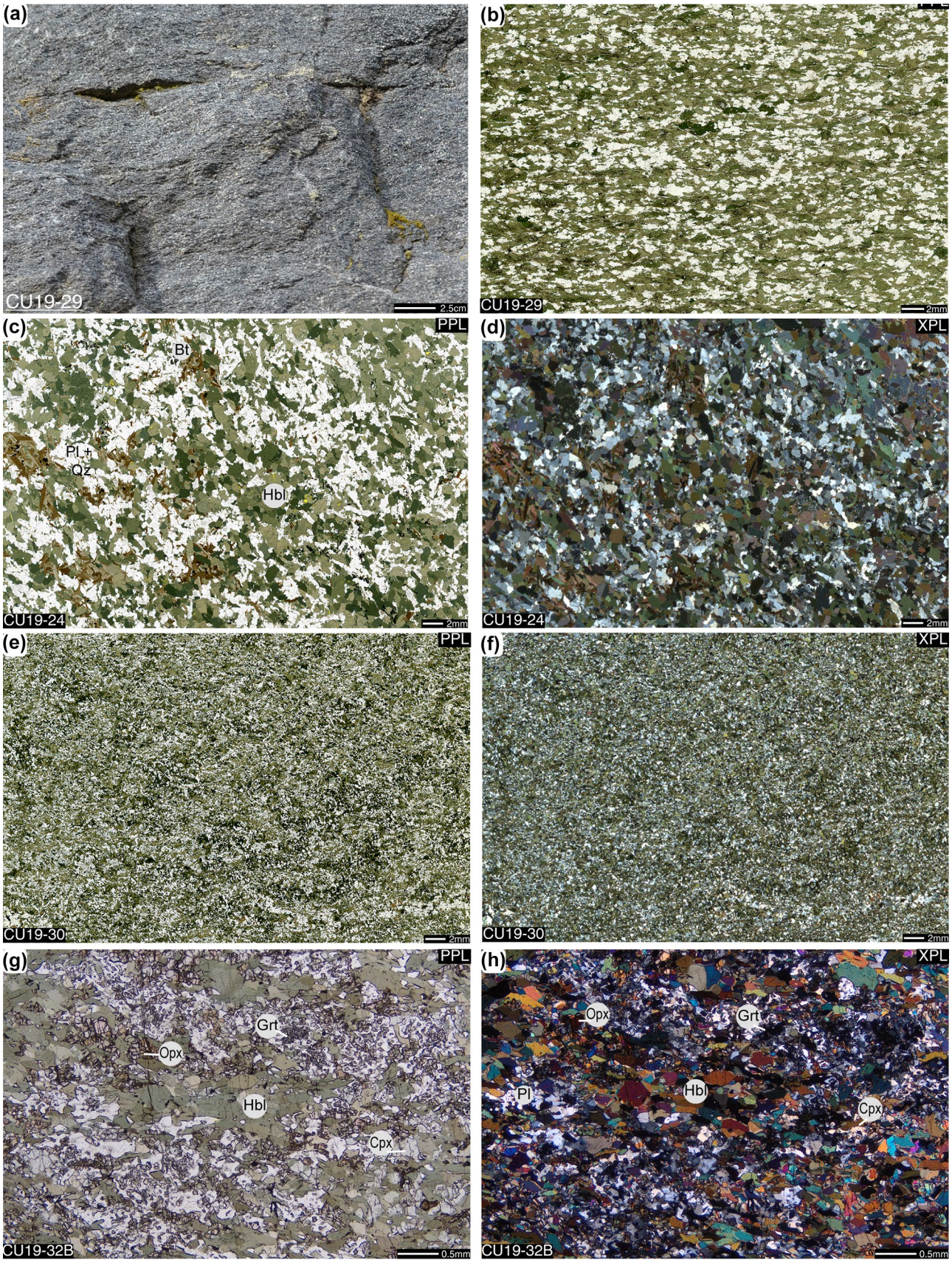
(a)
CU19-29
2.5cm
(b)
CU19-29
2mm
(c)
PPL
Bt
Pl +
Qz
Hbl
CU19-24
2mm
(d)
XPL
CU19-24
2mm
(e)
PPL
CU19-30
2mm
(f)
XPL
CU19-30
2mm
(g)
PPL
Grt
Opx
Hbl
Cpx
CU19-32B
0.5mm
(h)
XPL
Opx
Grt
Pl
Hbl
Cpx
CU19-32B
0.5mm

◂**Fig. 5** Non-migmatitic amphibolite (group C): field appearance, scanned thin sections, and photomicrographs. **a** Roadcut at Anderstorp exposing non-migmatitic amphibolite with a penetrative linear deformation fabric. **b** Thin section overview of the amphibolite from Anderstorp. **c–d** Scanned thin section overviews of undeformed amphibolite from Sandseryd, consisting of hornblende, plagioclase, quartz, and biotite. **e–f** Scanned thin section overviews of fine-grained amphibolite from Gransjön. **g–h** Photomicrographs (detail) of the fine-grained amphibolite from Bäck. Complex interlocking between fine-grained aggregates of garnet, pyroxene, plagioclase, and coarser hornblende crystals

In addition to the assessment for aggregate quality in road construction, rocks with good resistance to both abrasion and fragmentation, with M_{DE} values below 17% and LA value under 25%, meet the criteria for the highest quality suitable for railroad aggregates (Table 4; Fig. 10a, marked by a dashed line). All rocks in groups 0, A, B, and fine-grained amphibolites (samples 30 and 32B) fall within the class 1 category for railroad (Table 3; Fig. 10a).

The sampled rocks range in density between 3.00 and 3.25 g/cm^3 (Table 3). There is an overlap between the groups, but the individual groups dominate different parts of the density range. Amphibolites and migmatitic amphibolites of groups C and D dominate the lower range between 3.00 and 3.16 g/cm^3. The pristine and near-pristine rocks of group A are in the middle range (3.09–3.20 g/cm^3), while the higher range is represented by the high-pressure granulites of group E (3.12–3.25 g/cm^3). Figure 10b–c illustrate that the rocks with good resistance to both fragmentation (LA value < 25%; Fig. 10b) and wear/abrasion (M_{DE} value < 14%; Fig. 10c) have densities higher than 3.09 g/cm^3, while all rocks with densities below 3.06 g/cm^3 are class 3 material.

Interpretation and discussion

The technical test results (Fig. 10a) correlate almost perfectly with the degree of metamorphic recrystallization and metamorphic grain coarsening. Three principal groups are identified. The highest resistance to both fragmentation and wear is found in the pristine, near-pristine gabbro, and metagabbro with relict igneous texture. The second group comprises mafic granulite and fine-grained amphibolite, which both have good resistance to fragmentation but lower resistance to wear. The least resistance to wear and fragmentation are found in medium- to coarse-grained amphibolite, both migmatitic and non-migmatitic varieties. The metamorphic process involves changes in the mineral assemblage (primarily temperature-dependent) and texture (grain size and grain morphologies). Below ("The effects of petrographic parameters on technical properties of mafic rocks"), we first discuss the correlations of individual petrographic parameters. Thereafter ("The effects of metamorphism on gabbroic rocks and their technical properties" to "Implications related to extraction and use of mafic rock aggregates for road and railroad"), these properties are discussed in the context of geological and metamorphic setting and the implications for the use of mafic rocks as road aggregates.

The effects of petrographic parameters on technical properties of mafic rocks

The three petrographic parameters investigated in this study are (1) mineral assemblage and relative proportion of minerals, (2) grain size and grain size distribution, and (3) grain morphology and grain boundary complexity. Below, we discuss how these individual parameters appear to correlate with the technical test data.

Mineral assemblage and relative proportions of minerals

Apparent correlations between the modal contents of the major minerals (plagioclase, pyroxene, and hornblende) are illustrated in Fig. 11. Differences in major mineral contents are also accompanied by fundamental differences in both grain size and texture, factors that also strongly affect technical properties (cf. sections "Grain size and grain size distribution" and "Grain morphology and grain boundary complexity"). Therefore, the correlations with mineral contents must be interpreted with caution. In quartzofeldspathic rocks, high quartz and feldspar contents are commonly linked to a good resistance to fragmentation and therefore low LA values (cf. Pang et al. 2010; Ajagbe et al. 2015; Afolagboye et al. 2016; Adomako et al. 2021). For gabbroic rocks, however, this may not be the case. Despite relatively low amounts of quartz and feldspar (i.e., c. 20 modal-%, sample 13C), LA values are below 25%. On the other hand, our data indicate that higher amounts of plagioclase result in better resistance to wear (lower M_{DE}, Fig. 11b). There also appears to be a correlation between the amount of hornblende and the resistances to both wear and fragmentation, such that higher amounts of hornblende result in poorer technical properties. In addition, the absence of pyroxene appears to correlate with lower resistance to fragmentation (high LA value, Fig. 11a). However, these correlations may be apparent only, because of related differences in texture and grain size. Further systematic analysis would be needed to explore how the variation in mineral contents influences the technical properties.

The investigated mafic rocks contain less than 17 modal-% biotite, and there is no correlation between modal biotite content and LA or M_{DE} values (Fig. 11). Comparison of the technical properties of samples 27 and 35, both with very low contents of biotite, < 3 modal-% (Fig. 10), illustrates that biotite is not the main factor influencing the technical properties of this data set.

Neither is there a direct correlation between technical test results and the amount of garnet (not plotted). This

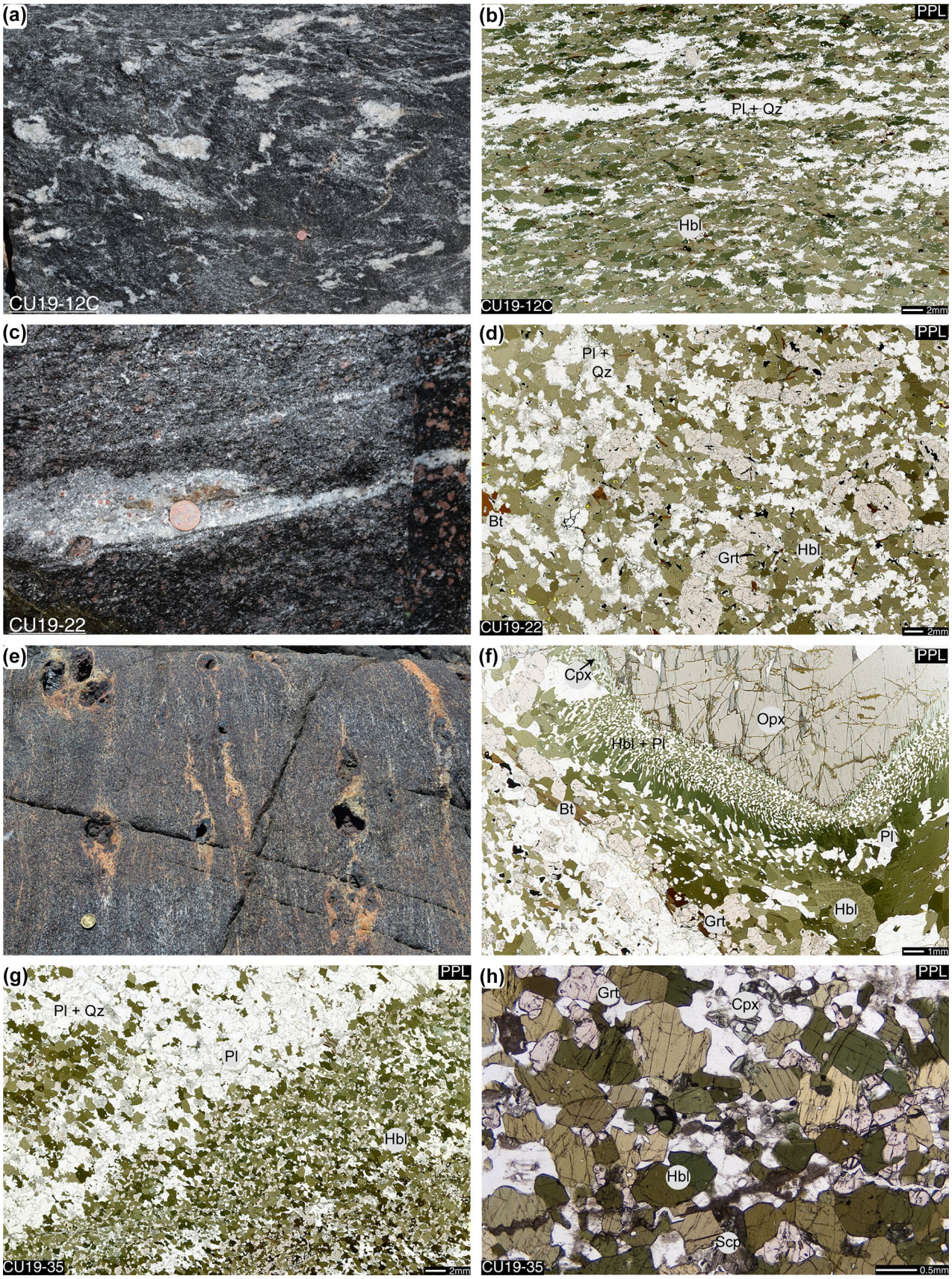
(a)
CU19-12C
(b)
PPL
Pl + Qz
Hbl
CU19-12C
2mm
(c)
CU19-22
(d)
PPL
Pl +
Qz
Bt
Grt
Hbl
CU19-22
2mm
(e)
(f)
PPL
Cpx
Opx
Hbl + Pl
Bt
Pl
Hbl
Grt
1mm
(g)
PPL
Pl + Qz
Pl
Hbl
CU19-35
2mm
(h)
PPL
Grt
Cpx
Hbl
Scp
CU19-35
0.5mm

◂**Fig. 6** Migmatitic amphibolite: field appearance, scanned thin sections, and photomicrographs. **a** Field appearance of patchy migmatite structure in garnet-poor amphibolite at the Kållerstad quarry. **b** Medium-grained planar fabric defined by hornblende-rich aggregates alternating with plagioclase- and quartz-rich domains. **c** Stromatic migmatite structure in garnet-rich amphibolite at the Nickelsbo quarry. **d** Photomicrograph of garnet-rich migmatitic amphibolite from Nickelsbo, made up of garnet, hornblende, and plagioclase, with subordinate biotite. The leucosome in the same rock is composed of plagioclase, quartz, and small amounts of fine-grained garnet. **e** Garnet-rich migmatitic amphibolite with orthopyroxene megablasts (partly weathered-out) in leucosome. Well-exposed locality at Stensjöstrand. **f** Thin section overview of well-preserved orthopyroxene megablast rimmed by fine-grained hornblende + plagioclase intergrowths, garnet, and locally clinopyroxene. **g** Thin section overview of mesosome + leucosome in garnet-rich migmatitic amphibolite with orthopyroxene megablasts. Hornblende and garnet dominate the mesosome, while the centimeter-wide leucosome bands mainly consist of antiperthite and scattered hornblende crystals. **h** Photomicrograph (detail) of garnet-rich, pyroxene, and scapolite-bearing mesosome from migmatitic amphibolite in Stockabacka locality

suggests that garnet does not influence the technical properties of mafic rocks, at least not up to ~ 30 modal-% (sample 13c, Fig. 8).

Grain size and grain size distribution

Grain size and grain size distribution are known to influence the resistance to fragmentation considerably in quartzofeldspathic rocks, for example, granitic rocks (Åkesson et al. 2001; Räisänen 2004; Lindqvist et al. 2007; Sajid et al. 2016; Hemmati et al. 2020; Urueña et al. 2021). Comparison of the amphibolite samples (group C) illustrates this effect (Fig. 8b). Samples 30 and 32B have a larger fraction of very fine grains compared to the three other samples in the same group, which is reflected in their lower LA values. It should be noted, however, that these two samples represent amphibolitized mafic granulites with relict metamorphic clinopyroxene and garnet. They also have more complex grain boundary morphology.

Noteworthy, the most coarse-grained rocks in the present data set are the pristine and near-pristine gabbro. Thus, for gabbroic and metagabbroic rocks, the correlation between fine-grained size and good technical properties, generally found for granitic rocks, does not seem to hold. This is because, for mafic rocks, the changes in both mineral contents ("Mineral assemblage and relative proportions of minerals") and—significantly—texture ("Grain morphology and grain boundary complexity") are more relevant.

Otherwise, for mafic rocks with similar mineral content and texture, we conclude that the grain size is an important factor for resistance to fragmentation and wear.

Grain morphology and grain boundary complexity

Pristine and near-pristine gabbroic rocks (groups 0 and A) have a pronounced interlocking (sub-ophitic) texture with coarse plagioclase forming an armoring network (Figs. 2 and 3). This texture correlates well with high resistance to fragmentation and wear. The straight grain boundaries of igneous plagioclase laths appear not to reduce the LA nor the M_{DE} values. Neither does the presence of very fine-grained coronas in near-pristine gabbro (group A, Fig. 3) appear to influence the technical properties negatively. The micro-scale textures within the coronas themselves (electron microscope, not illustrated) reveal that they have a complex interlocking texture which possibly have an armoring effect.

Rocks in group B have a relict sub-ophitic and interlocking texture, although most of the plagioclase and the dark minerals form fine-grained recrystallized aggregates (Fig. 4b–d). In hand sample, the plagioclase is white, in contrast to pristine and near-pristine gabbro that have dark plagioclase (cp. section "Group B: Metagabbro with relict igneous texture"). Sample 27 still preserves the original lath shape and twins (Fig. 4f). Despite significant metamorphic recrystallization and replacement of igneous pyroxene by metamorphic hornblende, the technical test results of group B rocks overlap those of groups 0 and A.

The texture of non-migmatitic and migmatitic amphibolite (groups C and D, Figs. 5 and 6) is different in all respects from the samples with pristine, near-pristine, and relict igneous texture (groups 0, A, and B). In these rocks, the igneous plagioclase laths are completely recrystallized and have been replaced by finer-grained aggregates of plagioclase and dark minerals with a more equigranular texture. Thus, the armoring effect of igneous plagioclase laths has been lost. We note that the amphibolite with a linear fabric, sample 29 (Fig. 5b), has poorer technical test values than the undeformed amphibolite, sample 24 (Fig. 5c), that resembles a pseudomorphosed igneous texture. However, additional samples would be needed for the evaluation of the effects of different strain states.

The fine-grained amphibolite samples, samples 30 and 32B, which are amphibolitized mafic granulites, both have complex grain boundary morphologies. Remnants of garnet and clinopyroxene have highly irregular shapes and so have the neighboring minerals (Fig. 5g, h).

The present data set show an overlap in technical properties of non-migmatitic amphibolite (group C) and migmatitic amphibolite (group D). It is notable, however, that migmatitic amphibolites are rarely (or never?) fine-grained. Moreover, the mesosome of these rocks tends to have a more granoblastic texture (Fig. 6). These two factors lead to lower resistance to fragmentation and wear, which explains why

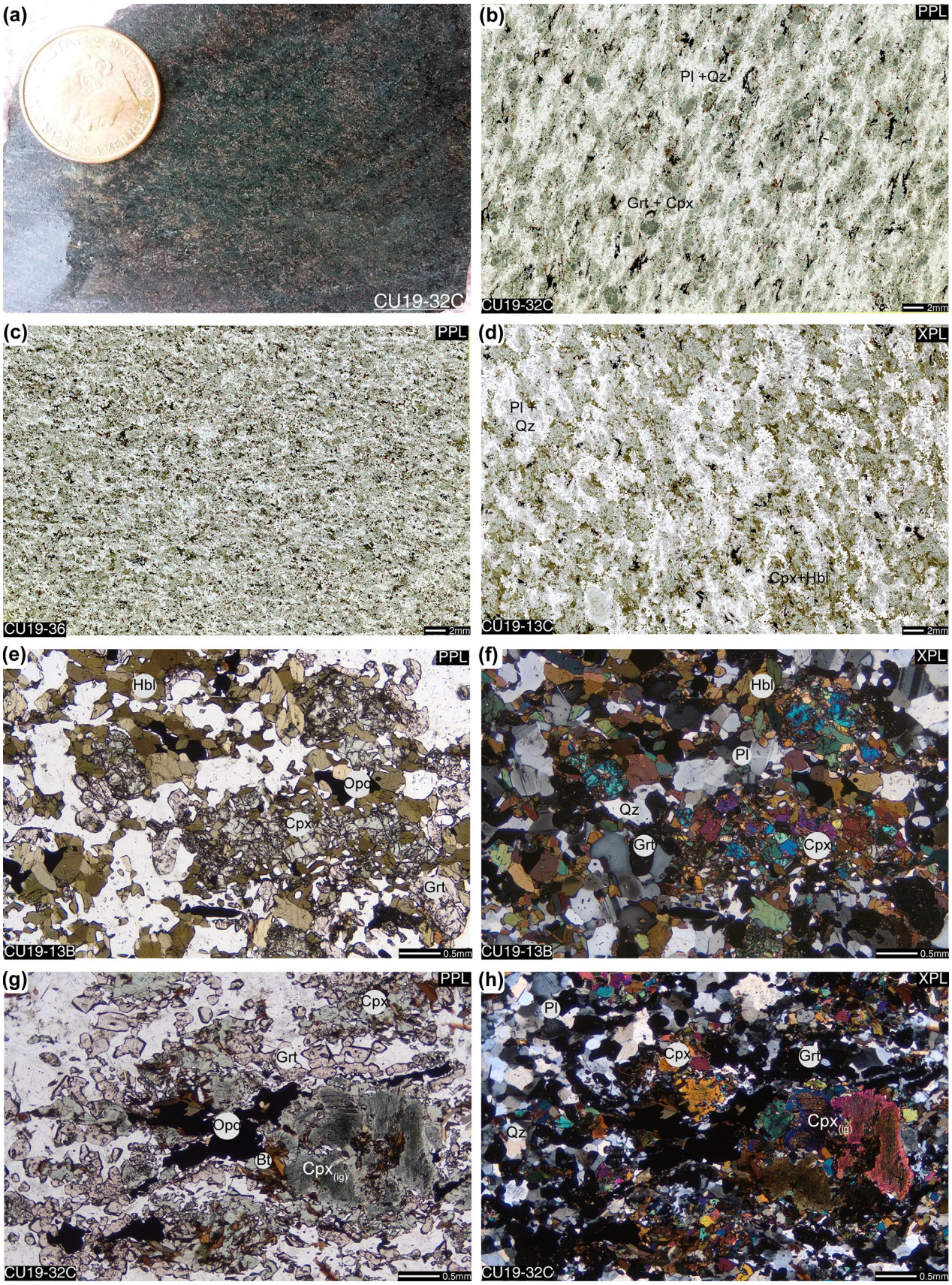
(a)
CU19-32C
(b)
PPL
Pl +Qz
Grt + Cpx
CU19-32C
2mm
(c)
PPL
CU19-36
2mm
(d)
XPL
Pl +
Qz
Cpx+Hbl
CU19-13C
2mm
(e)
PPL
Hbl
Opq
Cpx
Grt
CU19-13B
0.5mm
(f)
XPL
Hbl
Pl
Qz
Grt
Cpx
CU19-13B
0.5mm
(g)
PPL
Cpx
Grt
Opq
Bt
Cpx(ig)
CU19-32C
0.5mm
(h)
XPL
Pl
Cpx
Grt
Qz
Cpx(ig)
CU19-32C
0.5mm

◂**Fig. 7** Mafic granulite: field appearance, scanned thin sections, and photomicrographs. **a** Fine- to medium-grained mafic granulite with dark greenish pyroxene, reddish garnet, and light plagioclase. **b–d** Scanned thin section overviews showing variations in grain size and fabric of mafic granulite samples. These rocks are dominated by clinopyroxene, plagioclase, and garnet. Some have a domainal texture that is inherited from the primary medium- to coarse-grained igneous rock (**b** and **d**), albeit recrystallized and variably deformed. **e–f** Photomicrographs of a more hornblende-rich variety from the quarry at Rökla. Fine-grained clinopyroxene, hornblende, garnet, plagioclase, and opaques form a well-developed granoblastic texture. **g–h** Photomicrographs of clinopyroxene-rich variety from the quarry at Bäck, showing the large relics of igneous clinopyroxene ($Cpx_{[ig]}$) in the core and recrystallized clinopyroxene + garnet aggregates around

the migmatitic amphibolites dominates among rocks with low aggregate functionality.

Many mafic granulite samples (group E, Fig. 7) mimic the original igneous texture such that they preserve domains rich in plagioclase and dark minerals, respectively. Therefore, in many samples, the original igneous grain size can be approximately ascertained. In samples 13C and especially 32C (Fig. 7b), textural remnants of igneous clinopyroxene are preserved (clouded by abundant minute oxide inclusions). The rocks in group E have good LA values, below 22%, similar to groups 0, A, and B. One reason for this may be the relicts of an igneous interlocking texture. However, individual grains of metamorphic plagioclase, forming large aggregates, and garnet, forming string-like aggregates between felsic and mafic domains, are commonly granoblastic or near so. The granoblastic texture of the aggregates in these rocks does not seem to reduce the rocks' resistance to fragmentation. It may, however, influence the resistance to wear, which is lower than in groups 0, A, and B.

A final aspect is that microcracking caused by late brittle deformation may negatively influence the interlocking texture. In the present data set, the grain boundary and intracrystalline microcracks are preferentially formed in granoblastic aggregates. Nonetheless, the frequency of microcracking does not appear to correlate with the technical properties. Although sample 22, with the highest LA and M_{DE} values, has a high frequency of microcracks, other samples with the same microcracking pattern have better performance (Table 3). Moreover, samples with low and very low frequencies of microcracks have indistinct low or high LA and M_{DE} values (e.g., sample 27 low microcrack frequency and high performance or sample 35 low microcrack frequency and poor performance; Table 3).

The effects of metamorphism on gabbroic rocks and their technical properties

The present data set illustrates that metamorphosed gabbroic rocks may perform well or badly in technical tests (Fig. 10a) depending on the metamorphic conditions under which they have recrystallized. All the gabbroic rocks that preserve their igneous interlocking (sub-ophitic) texture are resistant to both fragmentation and wear (groups 0, A, and B). Where hydrated and recrystallized to medium- and coarse-grained amphibolite, however, the rocks perform poorly in the technical tests (groups C and D). The less hydrated metamorphosed rocks, i.e., mafic granulite dominated by metamorphic clinopyroxene + plagioclase + garnet, yield LA values in the same range as near-pristine gabbro, although their M_{DE} values are lower (group E).

Amphibolite samples 30 and 32B represent interesting examples (Fig. 10a). The textures in these rocks show that they were formerly richer in pyroxene and garnet but that they have been thoroughly amphibolitized. These rocks were likely fine-grained mafic granulites before the hydration. It is interesting to note that at least in these two cases, the resistance to fragmentation and to wear appears to have remained unchanged by the amphibolitization, possibly due to the preserved fine-grained size.

The striking petrographic difference between the samples in the present study cannot be explained by differences in whole-rock geochemistry but is the result of different metamorphic conditions. Metamorphism typically produces a combination of transformations of mineral assemblage, modal amounts of constituent mineral species, grain size, fabric, and texture. Below, we describe why geological processes yield the variations documented in the present sample set and infer that the variations primarily are a combined result of differences in metamorphic temperature and availability of hydrous fluid.

The metamorphic temperature and lithostatic pressure are usually considered to be the two primary controlling factors for the mineral assemblage formed. The metamorphic zone map (Fig. 1) illustrates the general increase in temperature within the Eastern Segment, inferred to increase from ~ 600 °C in the east to ~ 800 °C in the west (Möller and Andersson 2018). The variation in lithostatic pressure across the same zones is restricted and expected not to significantly influence the mineral assemblage in the present traverse. Throughout zones 3–8, lithostatic pressure is estimated at 9–11 kbar, which corresponds to depths of ~ 30–45 km. The lithostatic pressure is not yet quantitatively estimated for zones 1 and 2, but the metamorphic assemblages suggest mid- or low-crustal conditions, at depths exceeding 25 km.

The availability of hydrous fluid is also an important factor, particularly in metamorphosed igneous rocks. Depending on the amount of H_2O present, a mafic rock subjected to metamorphism at ~ 750 °C and 10 kbar will be transformed to either garnet granulite, garnet amphibolite, garnet-free amphibolite, or migmatitic amphibolite (cp. Palin et al. 2016). The presence of hydrous fluid will

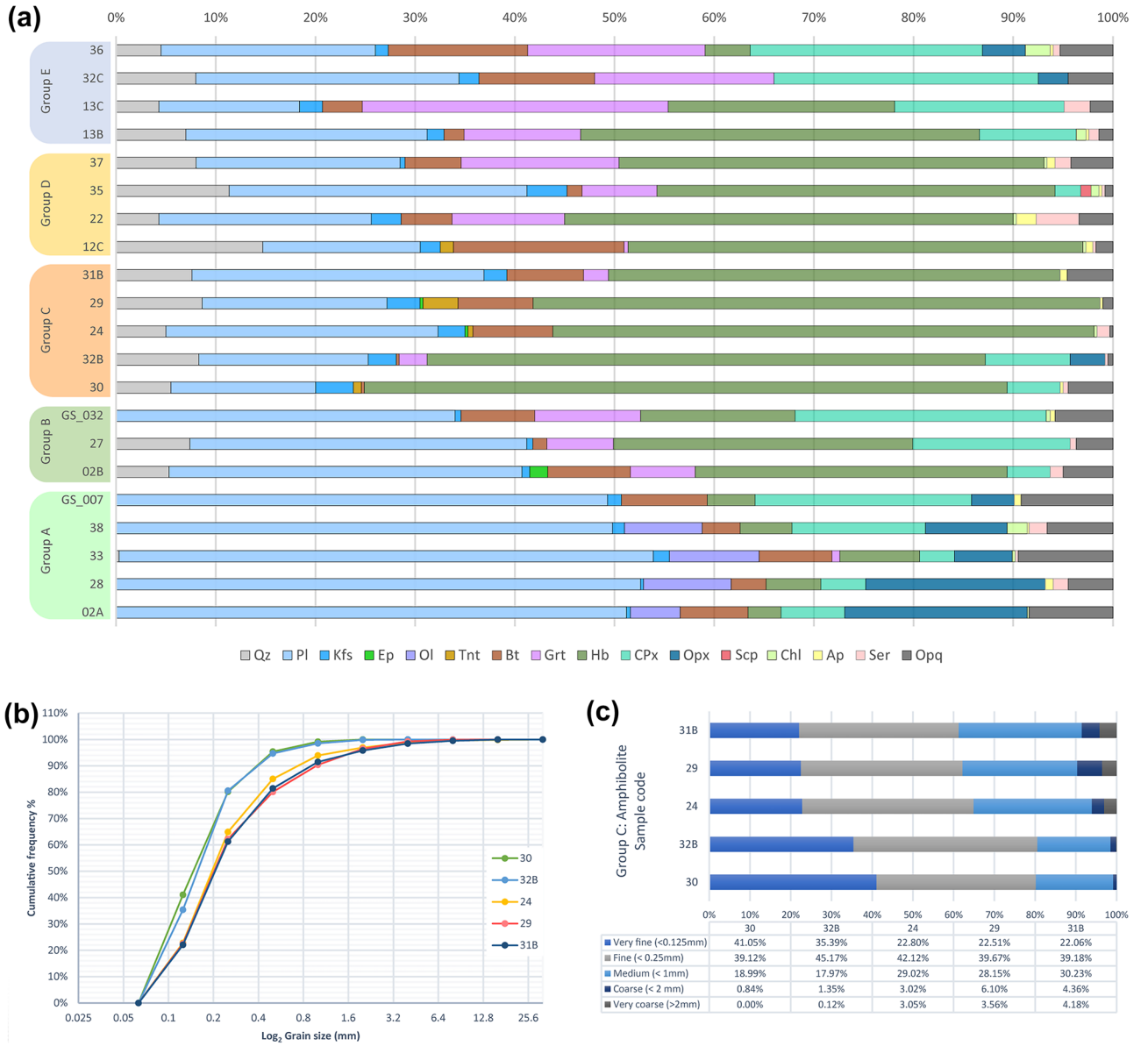

	30	32B	24	29	31B
Very fine (<0.125mm)	41.05%	35.39%	22.80%	22.51%	22.06%
Fine (< 0.25mm)	39.12%	45.17%	42.12%	39.67%	39.18%
Medium (< 1mm)	18.99%	17.97%	29.02%	28.15%	30.23%
Coarse (< 2 mm)	0.84%	1.35%	3.02%	6.10%	4.36%
Very coarse (>2mm)	0.00%	0.12%	3.05%	3.56%	4.18%

Fig. 8 Quantitative petrographic data. **a** Summary of mineral contents determined by point counting. Arrangement and color-coding of samples follow the subdivision of rock types in groups A–E. **b** Cumulative grain size distribution curves for samples in group C: Amphibolite. **c** Bar chart and data table showing the proportions of different grain sizes among the samples in group C

also enhance grain boundary diffusion and thereby the metamorphic reaction rate (i.e., metamorphic reactions go to completion), as well as the rates of recrystallization, metamorphic grain growth, and smoothening of grain boundaries.

In addition, deformation produces planar and/or linear structures and fabrics, which act as pathways for hydrous fluids, and induces metamorphic recrystallization. The distribution of deformation and associated hydrous fluid infiltration is typically heterogeneous in metamorphosed bedrock of igneous origin (cp. Austrheim 1987). Therefore, variations in mineral assemblage, grain size, and texture are common, even at scales less than a meter within the same rock type and at the same metamorphic pressure and temperature conditions. Thus, variable hydration states can occur within the same outcrop.

In the temperature range of zones 1–5, infiltration of hydrous fluid has steered both the degree of metamorphic recrystallization and the amount of amphibole formation in the rock. Where fluid infiltration was insignificant, recrystallization was much restricted and formed only very thin, very fine-grained coronas in the gabbroic rocks (group A). Where hydrous fluid was available but still limited, gabbro transformed to metagabbro with relict igneous texture (group B).

Table 3 Summary of technical test results: LA (%) = Los Angeles value, MDE (%) = micro-Deval value, and ρ (g/cm^3) = density. Classification for road aggregates following Mortensen and Göransson (2018; see Table 4). Modal classification based on whole-rock chemical composition for investigated samples and relative frequency of microcracks (detailed description in the text

Sampling group	Sample code	Locality	LA (%)	M_{DE} (%)	ρ (g·cm^{-3})	*Class*	Modal classification	Microcracks
Group 0: Pristine gabbro	SS1	Diabase quarry	17.0	7.3	n. d	2	n. d	n. d
	SS2	Diabase quarry	13.4	6.9	n. d	2	n. d	n. d
Group A: Near-pristine gabbro	02A	Mjogaryd quarry	16.6	8.1	3.14	2	Monzogabbro	Mid
	28	Herrestad incip. quarry	20.9	10.6	3.20	2	Gabbro	Low
	33	Målaskog roadcut	16.1	10.4	3.09	2	Syenogabbro	Low
	38	Bondstorp roadcut	15.3	7.4	3.09	2	Monzogabbro	Low
	GS_007	Gumlösa quarry NE of Hässleholm	15.8	8.0	n. d	2	n. d	n. d
Group B: Metagabbro w relict igneous texture	02B	Mjogaryd quarry	20.4	12.5	3.10	2	Syenogabbro	High
	27	Herrestad roadcut	15.7	8.3	3.13	2	Gabbro	Low
	GS_032	Sjunkaröd, SE of Hässleholm	12.6	6.8	n. d	2	n. d	n. d
Group C: Amphibolite	24	Sandseryd quarry	32.0	18.1	3.05	3	Alkali-gabbro	High
	29	Anderstorp roadcut	48.1	29.2	3.06	3	Gabbro	Low
	31B	Bökås quarry	25.9	35.5	3.10	4	Syenogabbro	Very low
	30	Gransjön roadcut	14.8	13.8	3.16	2	Gabbro	Very low
	32B	Bäck quarry	17.8	17.1	3.01	3	Monzogabbro	Very low
Group D: Migmatitic amphibolite	12C	Kållerstad quarry	33.6	23.5	3.03	3	Monzogabbro	High
	22	Nickelsbo quarry	70.6	35.5	3.12	4	Gabbro	High
	35	Stockabacka (old quarry)	31.0	21.7	3.00	3	Gabbro	Low
	37	Tippakull roadcut	39.7	28.1	3.14	3	Gabbro	n. d
Group E: Mafic granulite	13B	Rökla quarry	20.2	19.0	3.12	3	Gabbro	Mid
	13C	Rökla quarry	21.7	19.1	3.18	3	Gabbro	Mid
	32C	Bäck quarry	20.0	15.7	3.25	3	Gabbro	Very low
	36	Bårarp quarry	17.0	21.3	3.17	3	Gabbro	Very low

n. d. no data

Samples 02A and 02B (in Figs. 3 and 4) exemplify such a difference, in this case occurring over a few meters within the same gabbroic body. Where H_2O was abundant, the fluid caused complete amphibolitization and, from zone 4 and onwards, also induced partial melting (groups C and D). In zones 6–8, the temperature was high enough to induce near-complete recrystallization even without fluid infiltration. Consequently, very few metagabbroic rocks in zones 6–8 preserve remnants of igneous minerals even where only weakly hydrated (Fig. 7).

Implications related to extraction and use of mafic rock aggregates for road and railroad

In this study, we demonstrate that the performance of mafic rocks as road and railroad aggregates is directly related to the extent and mode of metamorphic recrystallization (cf. section "The effects of metamorphism on gabbroic rocks and their technical properties"). Consequently, successful prospecting relies on the understanding of the metamorphic character of these rocks. Although mafic rocks are not everywhere targeted for quarrying, they are commonly present as dikes, lenses, or layers in other rocks used for aggregate production. Depending on the volume and their metamorphic status, they may either improve or deteriorate the functionality of the bulk aggregate.

All rocks tested in this study have M_{DE} values above 7%, indicating a resistance to wear that is too low for use in all types of bound road layers, i.e., none of the samples classified as class 1 road aggregates. However, the pristine or weakly metamorphosed and the coronitic rocks (groups 0, A, and B) are well suited for most bound layers (class 2 road aggregate) and qualify as class 1 railroad aggregates (Fig. 10a).

Nonetheless, when the same rock type has been penetratively or near penetratively recrystallized to amphibolite and mafic granulite (groups C, D, and E), the resistance to wear is dramatically reduced and suitable for unbound road aggregates only (class 3). With LA values well below 25%, fine-grained amphibolites and mafic granulites retain a high

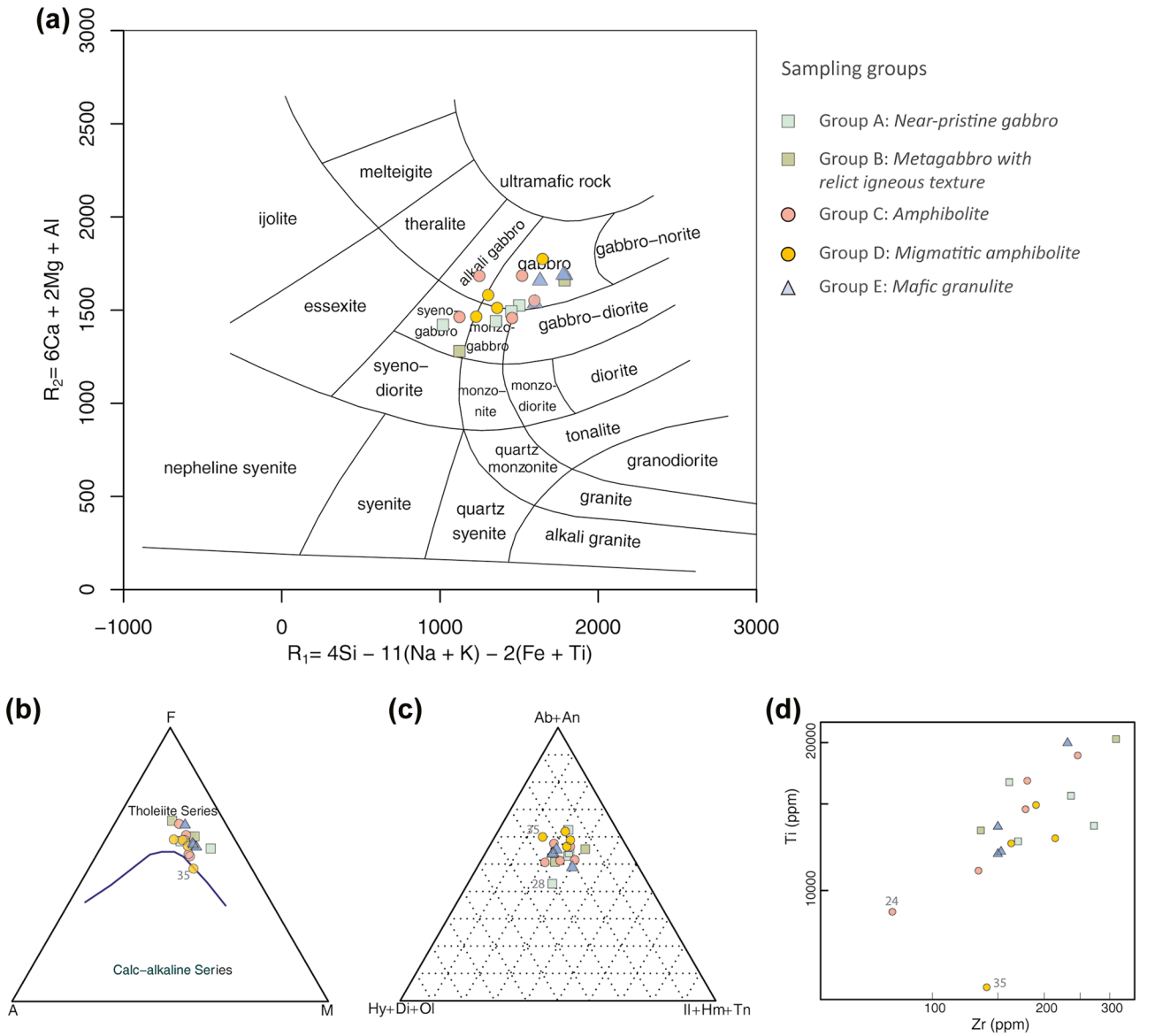

Fig. 9 Geochemical plots illustrating the compositional variation among the sampled mafic lithologies across the Eastern Segment. Color-coding follows the subdivision of rock types in groups A–E. **a** Geochemical classification based on the R1-R2 diagram (De la Roche et al. 1980). **b** AFM diagram for Tholeiite and Calc-alkaline series differentiation after Irvine and Baragar (1971). A = $Na_2O + K_2O$; F = FeO_{tot}; M = MgO. **c** Normative mineral proportions (after CIPW norm calculation). Hy + Di + Ol = Pyroxenes (hypersthene + diopside) and olivine; Ab + An = Plagioclase (albite + anorthite); Il + Hm + Tn = Fe-Ti oxides (ilmenite + hematite + rutile). **d** Zr vs. Ti diagram showing the correlation between two strongly incompatible trace elements

resistance to fragmentation, which is the requirement for a first-class railroad aggregate. Three out of four mafic granulite samples are unsuitable as railroad aggregates due to too low resistance to wear (M_{DE} value ≥ 17%; Fig. 10a).

Four samples of medium- to coarse-grained and migmatitic amphibolites show notably poor test results (LA value ≥ 40% and M_{DE} value ≥ 28%); samples 22 and 31B do not even meet the requirements for the production of any road or railroad aggregates (class 4 for both road and railroad). Such low resistance to wear and fragmentation is uncommon for crystalline rocks and is typically found in poorly consolidated sedimentary rocks, such as shales and deeply weathered rocks (Mortensen and Göransson 2018). Thus, metamorphosed mafic rocks have a wide variation in their functionality as road and railroad aggregates, but this variability in technical properties can be successfully predicted by documentation of the metamorphic state.

The conspicuous reduction in resistance to wear and fragmentation with progressive metamorphic recrystallization is accompanied by whitening of originally dark

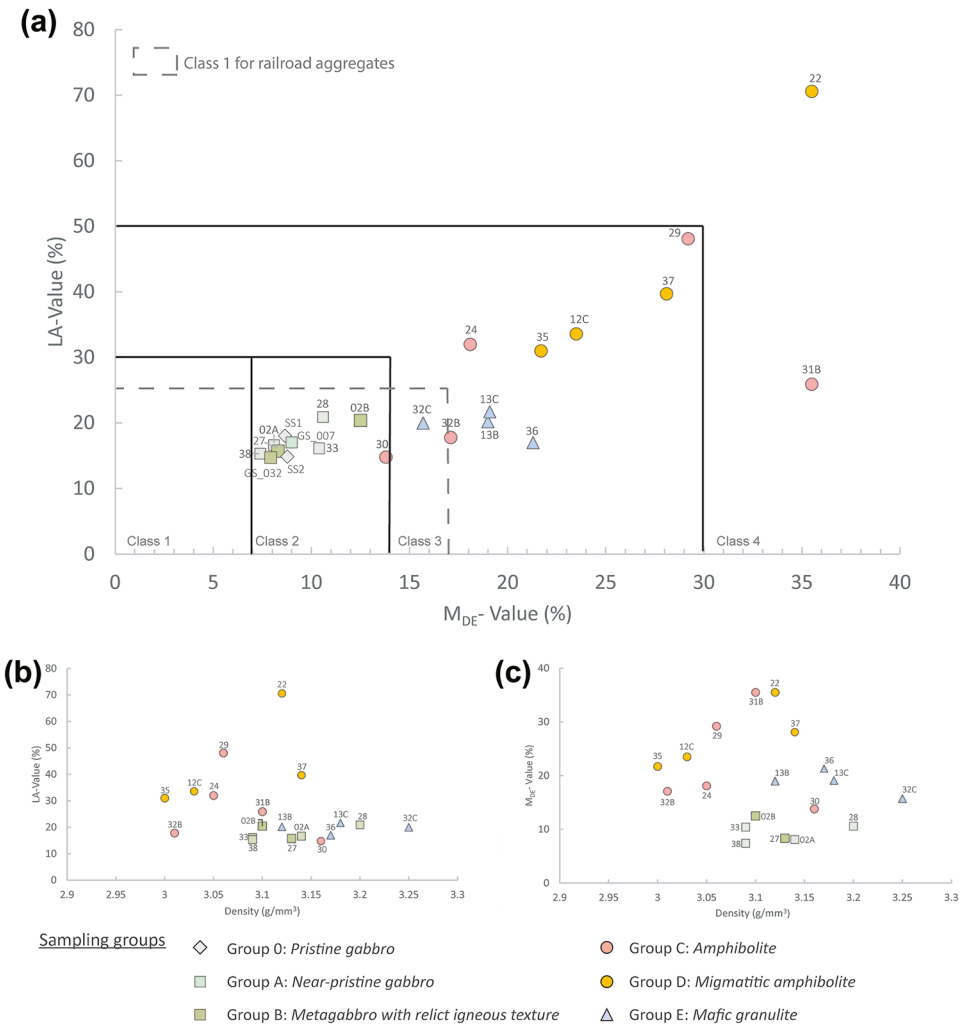

Fig. 10 Results from LA and M_{DE} tests and density for the investigated metagabbroic rocks (data in Table 3 and Online Resource 1). Color-coding follows the subdivision of rock types in groups A–E. **a** M_{DE} vs. LA diagram. Quality classification for road aggregates (black lines) and class 1 (dashed gray lines) for railroad aggregates, after Mortensen and Göransson (2018; Table 4). **b** Correlation diagram between density and LA value. **c** Density vs. M_{DE} value

plagioclase and loss of the igneous texture, readily notable in the field (cf. Figs. 3a–7a). Moreover, poor aggregate performance was found among all migmatitic amphibolites. The migmatitic rocks contain white veins easily distinguishable in the field (Fig. 6). Hence, metamorphic field mapping is a powerful tool for the prediction of the mafic rock aggregate properties. Understanding the metamorphic zoning of the crust at a larger scale can also be highly useful for the prediction of aggregate properties on a regional scale, for example, for the planning of large-scale

Table 4 Simplified classification based on technical values proposed by the Geological Survey of Sweden (SGU) for road and railroad aggregates quality assessment (after Mortensen and Göransson 2018)

Classification for road aggregates	**Class 1**	**Class 2**	**Class 3**	**Class 4**
Functionality	Highest quality, suitable for asphalt paving	Suitable for asphalt base courses	Only can be used in unbound layers	Inappropriate for use in road constructions
Los Angeles value	0–30%	0–30%	0–50%	> 50%
Micro Deval value	0–7%	7–14%	14–30%	> 30%
Classification for railroad aggregates	**Class 1**	**Class 2**	**Class 3**	**Class 4**
Functionality	Highest quality, suitable for ballast of superstructures and frost isolation layer	Suitable for ballast of substructures and frost isolation layer	Only can be used for frost isolation layer	Inappropriate for use in railroads
Los Angeles value	0–25%	25–30%	30–50%	> 50%
Micro Deval value	0–17%	0–17%	17–24%	> 24%

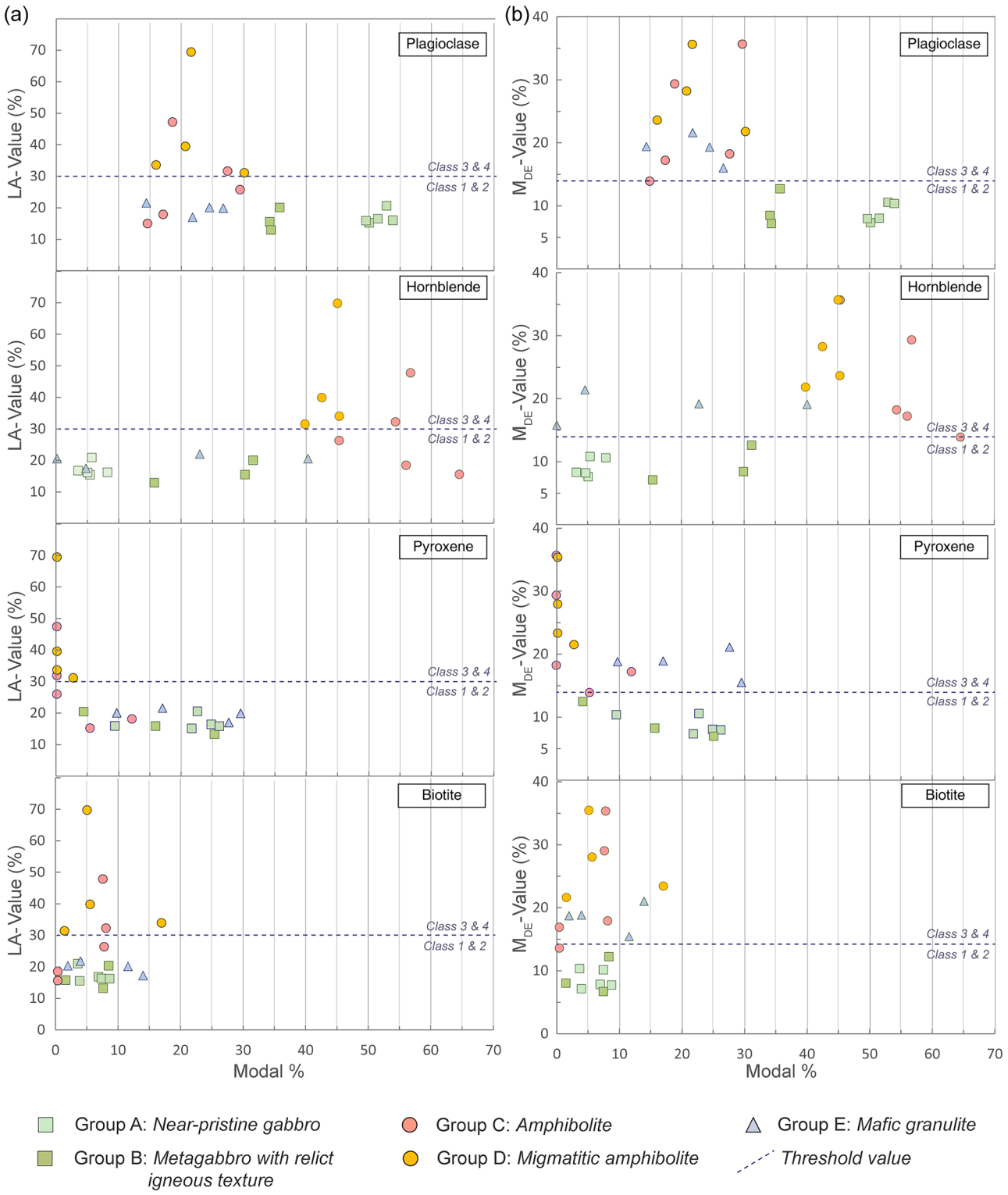

Fig. 11 Correlation diagrams between the mineral contents and technical test data. Color-coding follows the subdivision of rock types in groups A–E. The *x*-axis scale is kept for all relations to visualize variations in the proportions of each mineral. Note that some symbols can be overlapped. **a** Contents of major key minerals (plagioclase, hornblende, pyroxene, and biotite) vs. LA value. **b** Contents of major key minerals (plagioclase, hornblende, pyroxene, and biotite) vs. M_{DE} value

infrastructural projects and regional planning of material supply.

Even if gabbroic rocks can stay inert during metamorphism and their igneous mineral assemblages and textures can be preserved at relatively high metamorphic temperatures, an uneven infiltration and distribution of hydrous fluid will result in variation in the metamorphic recrystallization at the outcrop scale (e.g., Mørk 1985; Beckman et al. 2014). In the traverse studied here, heterogeneous recrystallization of mafic rocks in the metamorphic zones 2 and 3 involves transitions from well-preserved gabbro to foliated garnet amphibolite (Söderlund et al. 2004; Beckman et al. 2017). Such transitions can occur over a distance of a few meters in the same quarry or along a construction site (cf. Fig. 2 in Söderlund et al. 2004). In addition, several generations of mafic rocks in the same quarry may have widely variable aggregate properties. For instance, in some of the aggregate quarries in southernmost Sweden, amphibolitized Precambrian mafic rocks are crosscut by younger unmetamorphosed Permian dolerite. This example illustrates that sampling and testing of mafic rocks require good control of their metamorphic status.

Mafic vs. felsic rocks in aggregate production

The crushed rock road aggregate production in Sweden is almost exclusively focused on felsic rocks. Gabbroic rocks, such as those studied here, are commonly avoided. The main reason is that their higher density can negatively affect blasting and transport. Their high resistance to fragmentation, commonly much higher than the standard requirements, may also be problematic as it results in increased wear on crushing devices. In addition, the dark color can be disadvantageous for use in the wearing course. In some metamorphic zones, however, mafic rocks may have significantly better road aggregate properties than the felsic host rocks. Our tests of the resistance to wear and fragmentation of both felsic and mafic rock aggregates across eight different metamorphic zones illustrate this (this study and Urueña et al. 2021).

In metamorphic zones 0–1, both mafic and felsic rocks meet the requirements for bound layers in road construction. In zones 2–3, however, metamorphic recrystallization of the felsic rocks distinctly lower their resistance to fragmentation, and in zone 3, none of the felsic rocks has LA values below 30%, which is the threshold for use in bound layers. By contrast, all mafic rocks up to zone 3 have LA values below 22%, indicating much better resistance to fragmentation. The conspicuous lower resistance to fragmentation for the felsic rocks is likely because they lack an interlocking texture that is characteristic for the mafic rocks. The felsic rocks in zone 3 also have a much higher content of quartz, which has undergone coarsening and smoothening of grain boundaries (Urueña et al. 2021). Thus, in metamorphic zones 2 and 3, exploitation of mafic rocks may be more profitable than the use of felsic host rocks.

Another illustrative example is that felsic anhydrous high-grade gneisses in metamorphic zone 8 show high resistance to both wear and fragmentation (Möller and Andersson 2018; Urueña et al. 2021). Among the mafic rocks in these highest-grade metamorphic domains (zones 7–8), the migmatitic amphibolites have poor aggregate performance, while the mafic granulites have good resistance to fragmentation.

In summary, the different effects of metamorphism in mafic and felsic rocks must be considered for prospecting road and railroad aggregates in metamorphosed bedrock. Frequently, geological maps include sparse information on the metamorphic character of the mafic rocks. In most geological maps, different metagabbroic rocks such as those described in this study are commonly lumped together as metagabbro or amphibolite or in older maps as greenstones. We emphasize that more detailed mapping and classification of the metamorphic characteristics of mafic rocks are required for all exploitation of the bedrock.

Conclusions

Technical test data of metamorphosed gabbroic rocks show that the rock aggregate properties vary with metamorphic conditions, primarily temperature, and the availability of hydrous fluid. Petrographic data in this study show that:

- High resistance to fragmentation and wear strongly correlates with the preservation of the primary interlocking texture, i.e., the sub-ophitic texture, in which the network of plagioclase laths has an armoring effect, even when the primary igneous texture is only partially preserved. This is illustrated by recrystallized metagabbro with a relict igneous texture that gives LA values below 21%.
- The apparent positive correlation between modal contents of pyroxene and plagioclase and the resistance to fragmentation is at least partially linked to the preservation of interlocking igneous texture in poorly hydrated clinopyroxene-rich samples. A high amount of hornblende appears to correlate with decreased performance but is also linked to the rock texture, particularly to the loss of lath-shaped plagioclase and concomitant increase of granoblastic grains.
- The presence of garnet and biotite, both minerals occurring in low amounts only, did not influence the test values.
- Grain size appears to influence the technical values of non-migmatitic amphibolites, such that finer-grained

samples have better technical test values (LA and $M_{DE} < 18\%$). However, in the present data set, this correlation is again affected by more complex grain shapes and grain boundaries in the fine-grained amphibolite samples.

Overall, mafic rocks can perform well as aggregates for road and railroad, especially in terms of their resistance to brittle fragmentation. However, the variation in performance of mafic rocks in different modes of metamorphic recrystallization is large, ranging from high-performance aggregates suitable for road and railroad constructions to aggregates of a too poor performance to be used in any parts of road and railroad construction. This study validates that petrographic documentation and mapping of metamorphic recrystallization and texture are powerful tools for prospecting after high-performance mafic rock aggregates.

Supplementary information The online version contains supplementary material available at https://doi.org/10.1007/s10064-022-02718-8.

Acknowledgements The authors are thankful to Oscar Davies for doing the LA and M_{DE} analyses. We thank Scandinavian Stone and entrepreneurs in their quarries for providing technical data of pristine gabbro. Edward Hansen kindly provided his collection of thin sections of garnet amphibolite with orthopyroxene megablasts. The authors acknowledge perceptive and highly useful comments from two anonymous reviewers.

Author contribution All authors read and approved the final manuscript. Conceptualization: Charlotte Möller and Jenny Andersson. Methodology: Charlotte Möller, Cindy Urueña, Jenny Andersson, Jan Erik Lindqvist, and Mattias Göransson. Formal analysis and investigation: Cindy Urueña, Charlotte Möller, and Jenny Andersson. Writing - original draft preparation: Cindy Urueña, Charlotte Möller, and Jenny Andersson. Writing - review and editing: Charlotte Möller, Jenny Andersson, Cindy Urueña, Jan Erik Lindqvist, and Mattias Göransson. Funding acquisition and resources: Charlotte Möller, Jenny Andersson, Mattias Göransson, and Jan Erik Lindqvist. Supervision: Charlotte Möller, Jenny Andersson, and Jan Erik Lindqvist.

Funding Open access funding provided by Lund University. This project was supported by grant 36–1957/2017 from the Geological Survey of Sweden (SGU) to Charlotte Möller and by SGU-internal FoU-project 873012 to Jenny Andersson and Mattias Göransson.

Declarations

Competing interests The authors declare no competing interests.

References

Adomako S, Engelsen CJ, Thorstensen RT, Barbieri DM (2021) Review of the relationship between aggregates geology and Los Angeles and micro-Deval tests. Bull Eng Geol Environ 80:1963–1980. https://doi.org/10.1007/S10064-020-02097-Y/TABLES/8

Afolagboye LO, Talabi AO, Akinola OO (2016) Evaluation of selected basement complex rocks from Ado-Ekiti, SW Nigeria, as source of road construction aggregates. Bull Eng Geol Environ 75:853–865. https://doi.org/10.1007/S10064-015-0766-1/TABLES/3

Ajagbe WO, Tijani MA, Oyediran IA (2015) Engineering and geological evaluation of rocks for concrete production. Lautech J Eng Technol 9:67–79

Åkesson U, Lindqvist JE, Göransson M, Stigh J (2001) Relationship between texture and mechanical properties of granites, central Sweden, by use of image-analysing techniques. Bull Eng Geol Environ 60:277–284. https://doi.org/10.1007/s100640100105

Austrheim H (1987) Eclogitization of lower crustal granulites by fluid migration through shear zones. Earth Planet Sci Lett 81:221–232. https://doi.org/10.1016/0012-821X(87)90158-0

Beckman V, Möller C, Söderlund U et al (2014) Metamorphic zircon formation at the transition from gabbro to eclogite in Trollheimen-Surnadalen, Norwegian Caledonides. Geol Soc London, Spec Publ 390:403–424. https://doi.org/10.1144/SP390.26

Beckman V, Möller C, Söderlund U, Andersson J (2017) Zircon growth during progressive recrystallization of Gabbro to Garnet Amphibolite, Eastern Segment, Sveconorwegian orogen. J Petrol 58:167–188. https://doi.org/10.1093/petrology/egx009

Bingen B, Viola G, Möller C et al (2020). The Sveconorwegian Orogeny. https://doi.org/10.1016/j.gr.2020.10.014

Brander L, Appelquist K, Cornell D, Andersson UB (2011) Igneous and metamorphic geochronologic evolution of granitoids in the central Eastern Segment, southern Sweden. Int Geol Rev 54:509–546. https://doi.org/10.1080/00206814.2010.543785

Brander L, Söderlund U (2009) Mesoproterozoic (1.47–1.44 Ga) orogenic magmatism in Fennoscandia; Baddeleyite U-Pb dating of a suite of massif-type anorthosite in S. Sweden Int J Earth Sci 98:499–516. https://doi.org/10.1007/S00531-007-0281-0

De la Roche H, Leterrier J, Grandclaude P, Marchal M (1980) A classification of volcanic and plutonic rocks using R1R2-diagram and major-element analyses - its relationships with current nomenclature. Chem Geol 29:183–210. https://doi.org/10.1016/0009-2541(80)90020-0

Estifanos B, Yang C, Johansson L, Malmqvist KG (1997) A PIXE study of clouded plagioclase from southern Sweden. Nucl Instruments Methods Phys Res Sect B Beam Interact with Mater Atoms 129:83–91. https://doi.org/10.1016/S0168-583X(97)00211-5

Hansen E, Johansson L, Andersson J et al (2015) Partial melting in amphibolites in a deep section of the Sveconorwegian Orogen, SW Sweden. Lithos 236–237:27–45. https://doi.org/10.1016/j.lithos.2015.08.010

Hemmati A, Ghafoori M, Moomivand H, Lashkaripour GR (2020) The effect of mineralogy and textural characteristics on the strength of crystalline igneous rocks using image-based textural quantification. Eng Geol 266:105467. https://doi.org/10.1016/j.enggeo.2019.105467

Higgins MD (2006) Quantitative textural measurements in igneous and metamorphic petrology. Cambridge University Press, Cambridge

Irvine TN, Baragar WRA (1971) A guide to the chemical classification of the common volcanic rocks. Can J Earth Sci 8:523–548. https://doi.org/10.1139/e71-055

Lindqvist JE, Åkesson U, Malaga K (2007) Microstructure and functional properties of rock materials. Mater Charact 58:1183–1188. https://doi.org/10.1016/J.MATCHAR.2007.04.012

Lundqvist L (1996) 1.4 GA mafic-felsic magmatism in southern Sweden : a study of the Axamo Dyke Swarm and related Anorthosite-Gabbro intrusion. Göteborg University, Department of Geology, Earth Sciences Centre

Möller C, Andersson J (2018) Metamorphic zoning and behaviour of an underthrusting continental plate. J Metamorph Geol 36:567–589. https://doi.org/10.1111/jmg.12304

Möller C, Andersson J, Dyck B, Lundin IA (2015) Exhumation of an eclogite terrane as a hot migmatitic nappe, Sveconorwegian orogen. Lithos 226:147–168. https://doi.org/10.1016/J.LITHOS.2014.12.013

Mørk MBE (1985) A gabbro to eclogite transition on Flemsøy, Sunnmøre, western Norway. Chem Geol 50:283–310. https://doi.org/10.1016/0009-2541(85)90125-1

Mortensen G, Göransson M (2018) Bergkvalitet Skåne–beskrivning till bergkvalitetskartor över delar av Söderåsen, Kristianstadsområdet, Linderödsåsen och Romeleåsen. http://resource.sgu.se/produkter/k/k623-beskrivning.pdf. Accessed 22 Oct 2021

Palin RM, White RW, Green ECR et al (2016) High-grade metamorphism and partial melting of basic and intermediate rocks. J Metamorph Geol 34:871–892. https://doi.org/10.1111/JMG.12212

Pang L, Shaopeng WU, Jiqing Z (2010) Lu W (2010) Relationship between retrographical and physical properties of aggregates. J Wuhan Univ Technol Sci Ed 254(25):678–681. https://doi.org/10.1007/S11595-010-0069-0

Passchier CW, Trouw RAJJ (2005) Microtectonics, 2nd edn. Springer, Berlin, Heidelberg

Räisänen M (2004) Relationships between texture and mechanical properties of hybrid rocks from the Jaala-Iitti complex, southeastern Finland. Eng Geol 74:197–211

Rasband W (1997) ImageJ. U. S. Natl. Institutes Heal. Bethesda, Maryland, USA

Sajid M, Coggan J, Arif M et al (2016) Petrographic features as an effective indicator for the variation in strength of granites. Eng Geol 202:44–54. https://doi.org/10.1016/j.enggeo.2016.01.001

Söderlund P, Söderlund U, Möller C et al (2004) Petrology and ion microprobe U-Pb chronology applied to a metabasic intrusion in southern Sweden: a study on zircon formation during metamorphism and deformation. Tectonics 23:n/a-n/a. https://doi.org/10.1029/2003TC001498

Söderlund U, Isachsen CE, Bylund G et al (2005) U-Pb baddeleyite ages and Hf, Nd isotope chemistry constraining repeated mafic magmatism in the Fennoscandian Shield from 1.6 to 0.9 Ga. Contrib to Mineral Petrol 150:174–194. https://doi.org/10.1007/s00410-005-0011-1

Stephens MB, Wahlgren C-H (2020) Polyphase (1.9–1.8, 1.5–1.4 and 1.0–0.9 Ga) deformation and metamorphism of Proterozoic (1.9–1.2 Ga) continental crust, Eastern Segment, Sveconorwegian orogen. Geol Soc London, Mem 50:351–396. https://doi.org/10.1144/M50-2018-57

Tavares L, das Neves P (2008) Microstructure of quarry rocks and relationships to particle breakage and crushing. Int J Miner Process 87:28–41

Urueña C, Andersson J, Möller C et al (2021) Variation in technical properties of granitic rocks with metamorphic conditions. Eng Geol 293:106283. https://doi.org/10.1016/J.ENGGEO.2021.106283

Wahlgren CH, Heaman LM, Kamo S, Ingvald E (1996) U-Pb baddeleyite dating of dolerite dykes in the eastern part of the Sveconorwegian orogen, south-central Sweden. Precambrian Res 79:227–237. https://doi.org/10.1016/0301-9268(95)00094-1

Whitney DL, Evans BW (2010) Abbreviations for names of rock-forming minerals. Am Mineral 95:185–187. https://doi.org/10.2138/am.2010.3371